Kang *et al. Energy Mater* 2023;3:300043
DOI: 10.20517/energymater.2023.24

Energy Materials

Review

Open Access

Check for updates

Toward safer lithium metal batteries: a review

Shifei Kang[1,*,#], Jinmin Cheng[1,#], Weikang Gao[1], Lifeng Cui[2,*]

[1]Department of Environmental Science and Engineering, University of Shanghai for Science and Technology, Shanghai 200093, China.
[2]College of Smart Energy, Shanghai Jiao Tong University, Shanghai 200240, China.
[#]Authors contributed equally.

***Correspondence to:** Prof. Shifei Kang, Department of Environmental Science and Engineering, University of Shanghai for Science and Technology, 516 Jungong Road, Yangpu District, Shanghai 200093, China. E-mail: sfkang@usst.edu.cn; Prof. Lifeng Cui, College of Smart Energy, Shanghai Jiao Tong University, 665 Jianchuan Road, Minhang District, Shanghai 200240, China. E-mail: cui@usst.edu.cn

How to cite this article: Kang S, Cheng J, Gao W, Cui L. Toward safer lithium metal batteries: a review. *Energy Mater* 2023;3:300043. https://dx.doi.org/10.20517/energymater.2023.24

Received: 9 Apr 2023 **First Decision**: 4 May 2023 **Revised:** 12 Jun 2023 **Accepted:** 25 Jun 2023 **Published:** 9 Oct 2023

Academic Editor: Jia-Qi Huang **Copy Editor:** Fangling Lan **Production Editor:** Fangling Lan

Abstract

The energy density of conventional graphite anode batteries is insufficient to meet the requirement for portable devices, electric cars, and smart grids. As a result, researchers have diverted to lithium metal anode batteries. Lithium metal has a theoretical specific capacity (3,860 mAh·g^{-1}) significantly higher than that of graphite. Additionally, it has a lower redox potential of -3.04 V compared to standard hydrogen electrodes. These properties make high-energy lithium metal batteries a promising candidate for next-generation energy storage devices, which have garnered significant interest for several years. However, the high activity of lithium metal anodes poses safety risks (e.g., short circuits and thermal runaway) that hinder their commercial growth. Currently, modification of reversible lithium anodes is the primary focus of lithium metal batteries. This article presents conceptual models and numerical simulations that address failure processes and offer specific techniques to mitigate the challenges of lithium metal anodes, including electrolyte design, interface engineering, and electrode modification. It is expected that lithium metal batteries will recover and become a feasible energy storage solution.

Keywords: Lithium metal anodes, safety hazards, modification technology

INTRODUCTION

Lithium metal anodes are regarded as a “treasure” and the most attractive "ultimate anode" of the future

owing to their extraordinarily high specific theoretical capacity and low electrochemical potential. However, the problem of lithium metal anodes has remained unconquered for half a century. In recent years, researchers have made significant strides in lithium metal anode studies by leveraging research tools and nanotechnology. As a result, lithium metal anodes are once again becoming popular. New battery systems based on lithium metal anodes, such as Li-S and Li-O batteries[1], have the potential to generate specific energies exceeding 600 $Wh \cdot kg^{-1}$. Despite these advances, the practical use of lithium batteries is not yet promising.

For a long time, high reactivity, inhomogeneous deposition/dissolution, and unpredictable volume growth have been considered as the most frequent troubles faced by lithium metal anodes. In practical situations, lithium anode failures can be attributed to multiple factors, including low N/P ratios, reduced cell pressure, and accumulations of LiH[1]. To surmount the obstacles above, sundry methodologies have been suggested, including enhancing electrolyte additives, adjusting the interface between the electrolyte and lithium metal anode, constructing superior quality solid electrolytes, and designing three-dimensional (3D) anodes. A comprehensive discussion on these tactics shall be presented subsequently.

This review initially highlights the current issues and the microscopic mechanisms leading to battery failure. The "CHALLENGES AND MECHANISMS OF LITHIUM METAL BATTERIES" Section provides an in-depth discussion pertaining to electrolyte modification and electrode-electrolyte interface manipulation. It concludes by expounding on structural strategies for lithium anodes. Despite making significant strides in recent years, a noticeable disparity still persists between the performance of lithium metal batteries and the expectations of practical applications. In light of this, this review examines viable techniques for enhancing lithium metal batteries while providing recommendations concerning their commercialization.

CHALLENGES AND MECHANISMS OF LITHIUM METAL BATTERIES

The lithium anode, despite its potential, still faces significant challenges before it can be considered a competitive technology. These challenges take the form of both dynamic and static factors [Figure 1][2], with safety and cyclability being the most prominent among them. The dendritic formation is a common issue and has been identified as the primary cause of thermal runaway and explosion risks that arise from short circuits within the cells[3]. Therefore, achieving dendrite-free lithium (Li) deposition has become a crucial need. Additionally, high cyclability is essential in preventing low Coulombic efficiencies (CEs). Overcoming these obstacles requires a deep understanding of interfacial chemistry, Li deposition behaviors, and their correlations. This forthcoming discussion aims to provide a comprehensive analysis of the various challenges faced by lithium batteries while simultaneously proposing tailored optimization strategies to address them.

Lithium dendrite

Unrefined lithium metal is highly susceptible to dendritic growth when deposited unevenly on the current collector. Figure 2 illustrates each phase of dendritic growth. Once these dendrites reach a certain length, they can pierce through the separator, resulting in a direct connection between the positive and negative electrodes and ultimately leading to a short circuit [Figure 3E]. Furthermore, if a small branch of dendrites carries a substantial amount of current, an extraordinary amount of heat can be generated within the battery. In severe cases, these conditions may even cause explosions. These concerns regarding the lack of guaranteed safety present significant obstacles against the successful commercialization of these batteries.

The primary cause of mechanical failure in solid-state electrolytes (SSEs) is typically the high-stress field that arises from the electroplating of Li within pre-existing defects. This stress field drives crack propagation

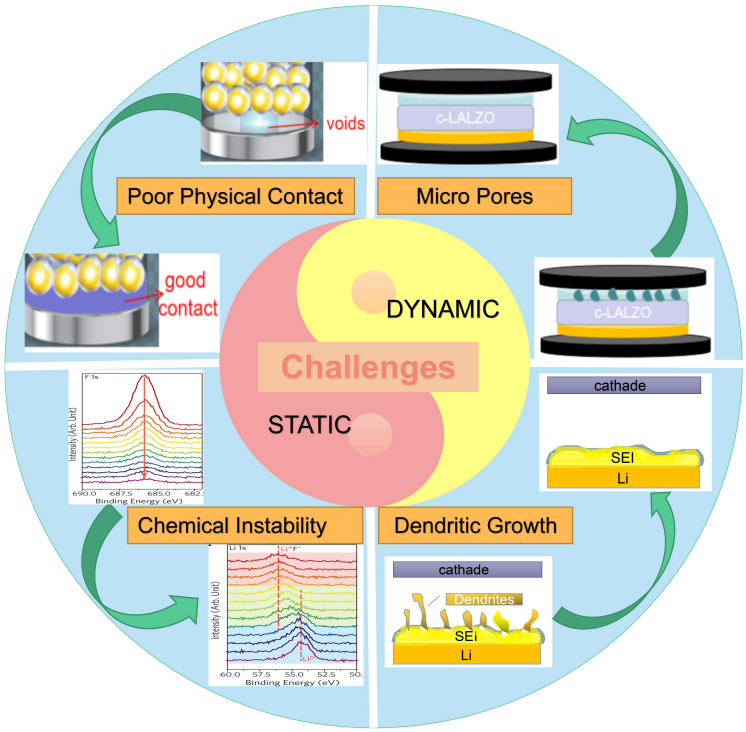

Figure 1. Interfacial problems of metal lithium anode[2] Copyright 2017, American Chemical Society.

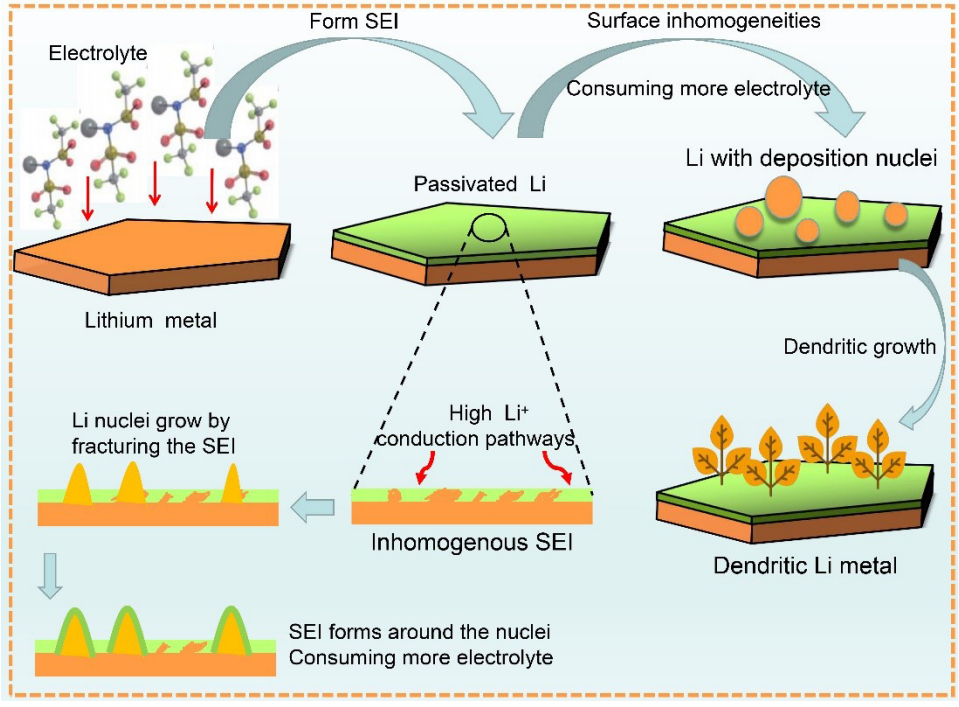

Figure 2. Schematic illustration of Li dendrite growth. Li: Lithium.

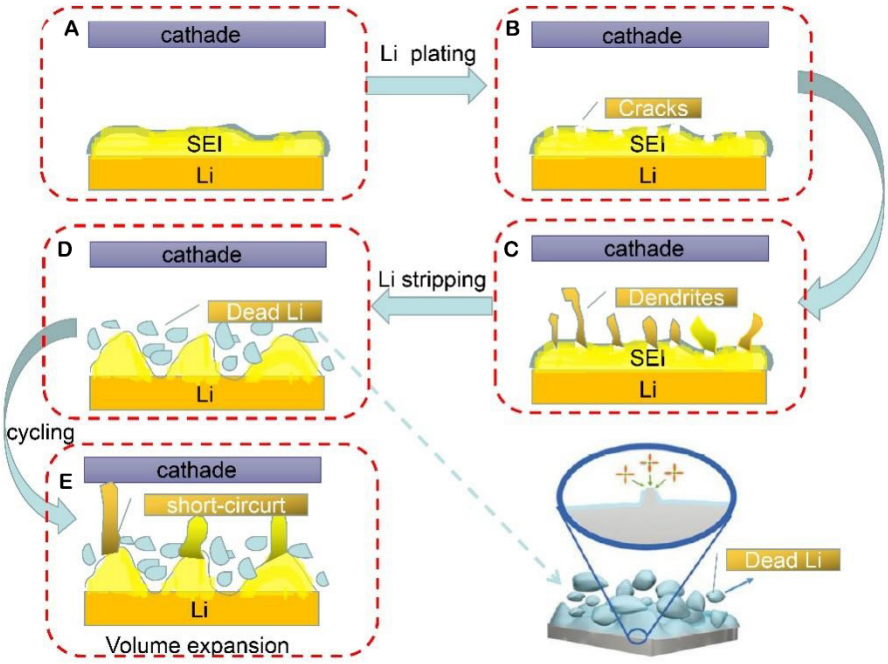

Figure 3. (A-E) Schematic illustration of lithium anode failure process.

throughout the electrolyte and leads to the growth of internal Li filaments. In severe instances, the filament may reach another electrode, resulting in an internal short circuit. To understand the role of interfacial defects on mechanical failures of SSEs, Xu *et al.* constructed an electro-chemo-mechanical model, which provides visual insights into the distribution of stress, relative damage, and crack formation during the electrochemical plating of Li in defects[4]. Geometry of interfacial defects was found as a dominating factor for a concentration of the local stress field, while semi-sphere defects delivered less damage accumulation at the initial stage and the longest failure time for disintegration of the electrolyte. The aspect ratio, a key geometric parameter of defects, was investigated to reveal its impact on electrolyte failure. In particular, pyramidic defects with low aspect ratios from 0.2 to 0.5 exhibit branched regions of damage that extend near the interface, leading to surface pulverization of the electrolyte. Conversely, for defects possessing a high aspect ratio exceeding 3.0, damage accumulation occurs primarily in the bulk electrolyte. The elucidation of such a correlation between interfacial defects and electro-chemo-mechanical failures in SSEs may offer invaluable guidelines for the design of interfaces in high-power-density solid-state lithium metal batteries. Clearly, mechanics play a more central role in solid-state batteries than in their liquid counterparts because of their rigid solid-solid interfaces[5]. The application of stresses during both the manufacturing and cycling of these batteries may give rise to substantial and often adverse effects on cell performance. During Li plating and stripping cycles, the manifestation of Li-induced stress at the anode/electrolyte interface is heavily influenced by the non-uniform morphology that encompasses heterogeneous nucleation and growth. Notably, each cycle inevitably induces a level of stress upon the battery, thereby causing irreparable damage to the solid electrolyte interphase (SEI) layer[6]. Furthermore, relative damage that arises from local high-stress events preferentially transpires within the region of significant electrolyte/Li interface fluctuations[7]. This damage is characterized by the formation of cracks [Figure 3A and B], which become the site for dendritic material growth [Figure 3C]. Inhomogeneous deposition of Li-ions tends to exacerbate the emergence of dendritic structures, and such behavior can be elucidated from both thermodynamic and kinetic perspectives[8]. Thermodynamically, metallic lithium undergoes repeated electroplating and stripping cycles during battery operation, inevitably leading to heat generation. However, the uneven distribution of

heat within the electrode compromises its interfacial uniformity and exacerbates dendrite formation[3]. Consequently, dendrite growth is nearly unavoidable. From a kinetic standpoint, dendrite formation in lithium is caused by many factors, including the surface status of lithium and the anodic electric field. The presence of surface defects in Li_2O, Li_2CO_3, and pristine lithium makes them more susceptible to uneven deposition[9]. Typically, when lithium metal with surface defects is immersed into an electrolyte, rapid reactions occur on the metal surface, forming an uneven SEI layer. The unevenness of the SEI layer leads to an uneven current distribution, causing non-uniform deposition of lithium after multiple battery cycles[10]. The uneven current distribution and uneven SEI surface layer promote mutually in a vicious cycle, resulting in a significant decrease in cell Coulomb efficiency and difficulty in ensuring battery safety.

Apart from the above scenario, non-uniform electric fields caused by ion concentration gradients or unstable electrolyte concentrations can also lead to dendrite growth. Reportedly, the transport of Li^+ is more challenging than that of anions due to the abundant solvent molecules in the solvent sheath surrounding Li^+[11]. As a result, the concentration of anions adjacent to the cathode quickly decreases to zero, forming a space-positive charge region. This space charge domain generates a local electric field that triggers dendrite growth. To counteract this phenomenon, electrolytes with better ionic conductivity and reduced anion mobility are employed to mitigate anion depletion near the electrode/electrolyte interface[12], consequently suppressing the nucleation of dendrites. Through live scanning electron microscope observations, Dollé *et al*. made the astute observation that the evolution of lithium from a mossy to a needle-like structure was contingent on the increase in current density[6]. Furthermore, based on meticulous calculations and rooted in the mechano-electrochemical phase field model, it was established that Li deposition on the anode was smoother within a particular range when the battery underwent heightened pressure[3]. Specifically, the lower pressure endured by the lithium anode of the pouch battery ultimately determined its inferior performance. Yet, the exertion of excessive pressure ran the risk of fracturing dendrites at their roots[13], which caused a corresponding loss of capacity. While the appropriateness of pressure levels plays a crucial role in attaining optimal performance in lithium metal batteries, the underlying mechanics are multifaceted and nuanced.

As reported, lithium dendrites are highly susceptible to formation under low surface energy and high migration energy. High temperatures can reduce surface migration barriers and promote ion diffusion, effectively reducing nucleation density and forming smoother Li deposition. Consequently, adjusting temperature can alter the nucleation and growth behavior of lithium. The ultimate state of Li deposition is highly dependent on its initial shape. The most common morphologies are needle-like, moss-like, and dendritic shapes, and lithium dendrite is widely used to describe the above uneven deposition morphology[14]. Dendrite nucleation involves multiple disciplines, including chemistry, electrochemistry, crystallography, molecular dynamics, and thermophysics, which render a single model insufficient in explaining this phenomenon. While many high-potential metals, such as Zn, Cu, and Ni, also produce dendrites during electrochemical deposition, their dendrite growth mechanism has been thoroughly studied. However, the excessively low reduction potential of metal Li-ions leads to a dendrite growth mechanism that is fundamentally different from that of other metals. As a result, the problem of lithium dendrites remains unresolved, and the theory of dendrite growth requires further investigation. This review will follow various schemes for the suppression of lithium dendrites.

Although various strategies are committed to inhibiting the growth of lithium dendrites, dendrite growth is still inevitable thermodynamically. Also, lithium dendrites grow to a certain extent and then spontaneously fall off to form ineffective metal lithium, which can no longer participate in subsequent battery reactions [Figure 3D]. The invalid lithium metal is customarily called “dead lithium”.

Dead lithium

Dead lithium refers to the irreversible capacity loss experienced by batteries[15]. Recent studies suggest that the CE of Li deposition/dissolution in nonaqueous electrolytes is significantly lower than 99.2%[16], primarily due to the uncontrolled formation of dendrites and subsequent accumulation of dead lithium. Therefore, a thorough comprehension of the underlying mechanisms behind the formation of dead lithium is necessary. Figure 3A-E illustrates the detailed formation mechanism of dead lithium and the consequent failure process of lithium batteries. Notably, dendrite necks with larger curvature tend to accumulate at a higher electron density and exhibit faster rates of lithium dissolution[17]. This often results in dendrite fractures at these sites. Subsequent exposure of the newly-exposed lithium to the surrounding electrolyte initiates repeated reactions that continuously consume it, reducing battery capacity. Empirical studies demonstrate that dead lithium is directly attributed to internal stress and current distribution within the battery. For instance, uneven current distribution in the microporous collector can lead to detachment of the lithium metal located in the center of the pore channel from the porous skeleton. Scholars have proposed to adjust porous collector pore sizes and current distributions to minimize the incidence of "dead lithium"[18]. Notably, among the myriad of challenges identified over the years, high chemical reactivity and volume fluctuations are often regarded as two fundamental hurdles. These issues are intensified by SEI failures, which exacerbate electrochemical side reactions, resulting in the formation of abundant dendrites and dead lithium. This ultimately leads to significant volume expansion within the anode, posing considerable safety concerns and contributing to a marked decline in CEs.

Volume expansion of lithium anode

In the realm of electrochemistry, it is a widely accepted fact that volume fluctuations are ubiquitous in electrode materials during charge and discharge cycles. Even commercial graphite electrodes, which are commonly used in batteries, experience up to 10% volume fluctuations. This phenomenon becomes more pronounced in the case of lithium metal. Notably, a commercially viable single-sided electrode must possess an area capacity of 3 $mAh \cdot cm^{-2}$, which, for lithium, will result in a volume change of 14.6 μm[6]. This value is bound to escalate in the future, implying that the lithium interface will move by tens of microns during cycling.

The non-uniform distribution of internal stress generates cracks in the SEI layer, leading to the growth of dendrites[19]. These loose dendritic structures exacerbate the volume expansion of the lithium metal anode[20] [Figure 3E]. Dendrites and volume expansion jointly contribute to the formation of a vicious cycle that further disrupts the electrode/electrolyte interface. After several battery cycles, a substantial amount of dead lithium builds up on the electrode, and this accumulation increases the anode thickness, thus intensifying battery resistance.

In the realm of applied lithium battery technology, anode expansion can be attributed to the insult and pulverization of LiH. Xu *et al.* studied a battery featuring an ultra-thin lithium anode and a high-load cathode ($LiCoO_2$) and found that the proportion of LiH by-products on the anode surface rose dramatically from 0.74% to 16.55% after 20 cycles[4]. The content of LiH on the anode surface is reportedly inversely related to battery life, and the volume of lithium metal anodes without any supporting structure significantly changes during the electrochemical process. There is no experimental evidence to confirm that high current density (1.5 $mA \cdot cm^{-2}$) directly causes battery failures[21]. However, at high current density, the expansion of the lithium/electrolyte interface region leads to the formation of more SEI components, which curtail contact between lithium particles and bestow a porous structure. This porous structure has a larger specific surface area and reduces electrolyte wettability at the interface, resulting in greater interfacial impedance. Accordingly, this increase in the interstitial resistance of the porous SEI is considered as the actual cause of ultimate failure in lithium metal batteries.

Corrosion of lithium anode

Due to its high negative redox potential, lithium spontaneously reacts with the electrolyte to form a detrimental SEI layer[22]. During cycling, this unstable SEI continuously fractures, giving rise to freshly-exposed lithium, which repeatedly reacts with the electrolyte. Continuous consumption of the electrolyte and electrochemical corrosion of metallic lithium lead to a low CE and gradual capacity decay[23,24]. The three primary factors affecting the reactivity of lithium and electrolytes are the electronic structure, the strength of the electrolyte, and the stability of the SEI. Moreover, the viscosity of the electrolyte can affect the corrosion rate of lithium. Reports suggest that low-viscosity dimethoxyethane and tetrahydrofuran perform poorly in lithium stability compared to propylene carbonate and ethylene carbonate. A robust SEI can prevent fresh lithium exposure, which is the primary factor influencing lithium corrosion. The composition and properties of the SEI are closely related to the electrolyte composition. For instance, an unstable SEI is formed on the surface of a lithium metal battery electrode with a conventional ethylene carbonate electrolyte. In contrast, a fluorine-substituted cyclic carbonate electrolyte yields a chemically stable LiF-enriched SEI on the surface of a lithium anode[25]. Therefore, adjusting the electrolyte composition to enhance the stability of the SEI can mitigate lithium corrosion.

The causes of battery failures have not been fully explained, which is not conducive to subsequent battery optimization. Hence, understanding the underlying mechanism of battery failures must be pursued relentlessly to improve battery performance. An exhaustive array of factors is thought to contribute to the failure of lithium metal batteries. Figure 4 depicts the current state of battery technology, highlighting the inherent complex relationships therein. This article delves into the specific strategies that can be employed to address these issues.

STRATEGIES TO SOLVE ISSUES OF THE LITHIUM ANODE

Studies show that external barriers can stabilize the lithium anode, inhibiting the formation of lithium dendrites, dead lithium, and expansion. Monroe and Newman[26] suggest that the growth of lithium dendrites can be entirely suppressed if the shear modulus of the electrolyte doubles that of the lithium metal. Inorganic solid electrolytes typically exhibit high mechanical strength, effectively impeding the formation of lithium dendrites and preventing the emergence of dead lithium. However, the solid electrolyte exhibits inadequate contact with the lithium metal anode, as scanning electron microscopy(SEM) shows that only point contacts exist on the interface[27], drastically increasing interface impedance. The subsequent uneven reaction seriously undermines the electrochemical performance of the solid-state battery[28]. Specific interface engineering strategies have been proposed to address the chemical instability and poor physical contact at the electrolyte-electrode interface. For example, the introduction of various ultrathin coatings on the surface of SSEs has been studied to enhance the wettability of lithium. Zheng *et al.* utilized atomic layer deposition (ALD) to uniformly deposit ultrathin Al_2O_3 onto the interface of lithium metal and $Li_7La_{2.75}Ca_{0.25}Zr_{1.75}Nb_{0.25}O_{12}$ (LLCZN) solid electrolyte[29]. The Al_2O_3 coating was shown to vastly improve the wettability of lithium metal and LLCZN. The boundary resistance at room temperature was reduced from 1,710 to 34 Ω cm^{-2}, while the lithiated alumina interface effectively facilitated the transport of Li-ions between lithium and LLCZN, stimulating the uniform deposition of Li-ions on the surface of lithium metal. In addition to the above approaches, battery cycle stability can be secured by modifying electrolyte properties and constructing optimized 3D structural frameworks. The 3D structure framework can provide adequate space for subsequent deposition and ensure an effective ion/electron transport path, mitigating stress accumulation and stabilizing the mechanical structure of the solid electrolyte. While the separator is not an active component during battery charging or discharging, its characteristics play a critical role in determining battery performance and durability. Therefore, modifying the separator is considered within the scope of battery optimization strategies. Figure 5 presents various optimization strategies, which will be elaborated on in what follows.

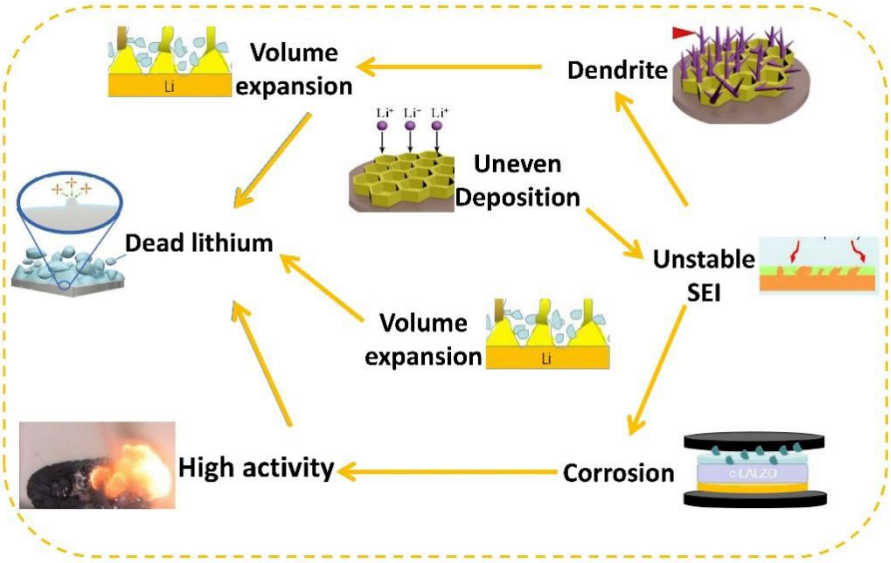

Figure 4. The correlations among anode issues.

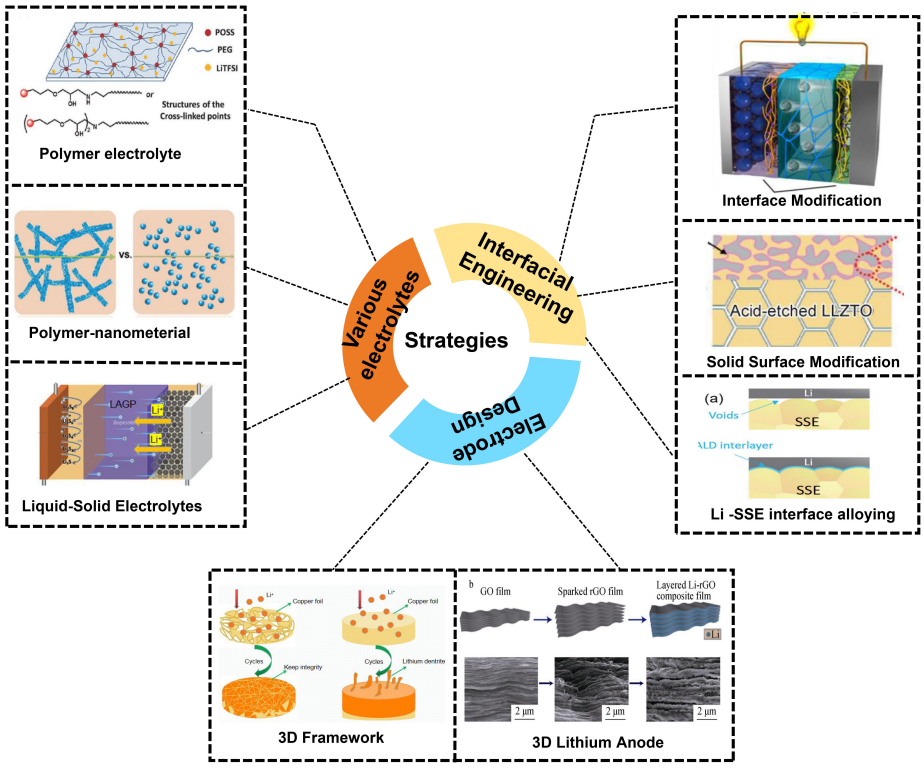

Figure 5. Various strategies for battery configuration optimization[30]. Copyright 2020, American Chemical Society.

VARIOUS ELECTROLYTES

The following discourse delves into the unique advantages of various electrolytes in depth. Initially, polymer electrolytes are introduced, which exhibit high flexibility and mechanical strength.

Polymer electrolytes

Metallic lithium batteries, known for their high energy density, are promising for a wide range of applications. However, due to the complexity of multiple reactions inside the battery and the impact of factors such as high temperature, overcharging, and discharging, metallic lithium batteries are prone to thermal runaway, explosions, and other safety issues. In this regard, the application of polymer electrolytes can significantly improve the safety of metallic lithium batteries. Firstly, compared with traditional liquid electrolytes, polymer electrolytes have lower volatility and higher melting points, thereby reducing the risk of thermal runaway inside the battery. Secondly, polymer electrolytes have higher chemical stability, which prevents harmful substances generated by internal reactions from damaging the electrolyte, thereby reducing the production of gas and sediment in the battery and lowering pressure accumulation. Additionally, polymer electrolytes can achieve fast ion transfer and low resistance by changing their molecular structure, further improving battery performance and safety.

Polymer electrolytes have been identified as a promising solution to the mechanical suppression of lithium dendrites. Various polymer electrolytes, such as copolymers, cross-linked polymers, and polymer/nanoparticle composites, have been developed to integrate high ionic conductivity with sufficient shear modulus to prevent the formation of lithium dendrites[30]. Polymer electrolytes have been widely studied as they maintain high electrochemical stability, flexibility, and mechanical durability, specifically focusing on solid polymer electrolytes (SPEs) in this discussion.

Among SPEs, the polyethylene oxide (PEO)-based electrolyte has garnered significant attention due to its remarkable solubility of Li-ions and high chain flexibility[31]. The ethylene oxide (EO) functional group can coordinate with Li^+ to form an EO-Li^+ complex, enabling the Li-ions to traverse along the long polymer chain of PEO. However, the crystalline structure of PEO impedes ionic conductivity at room temperature, although this obstacle can be overcome by raising the temperature. Nevertheless, this approach can also reduce the shear modulus of the electrolyte. Studies show that the growth of lithium dendrites can be entirely prevented when the shear modulus of the electrolyte is twice that of lithium metal[26]. Consequently, there is a contradiction between shear modulus and ionic conductivity. The shear modulus of PEO homopolymer is about four orders of magnitude lower than that of lithium metal, which is insufficient to entirely prevent dendritic growth. In pure PEO, the rate of lithium dendrite growth is ten times faster than that in block copolymers. These findings suggest that the shear modulus of the electrolyte influences Li deposition.

Poly(vinylidene fluoride-co-hexafluoropropylene) (PVDF-HFP) is a popular polymer matrix for gel polymer electrolytes, but its stiffness is negligible. To address this issue, Tu *et al.* developed a laminated electrolyte/separator material by placing a nano-porous Al_2O_3 sheet between PVDF-HFP membranes[32]. The resulting electrolyte/separator has an ionic conductivity of over 1 $mS{\cdot}cm^{-1}$ and high mechanical strength at room temperature. This design effectively stabilizes lithium metal batteries and prevents cell short circuits. Incorporating polymer electrolytes with nanostructured ceramics is a common method to enhance the stiffness of the electrolytes for dendrite suppression. For instance, SiO_2 hollow nanospheres were utilized to provide a mechanically strong scaffold for the gel polymer electrolyte as a composite solid electrolyte with a high ionic conductivity of 1.74 $mS{\cdot}cm^{-1}$ and enhanced safety features such as non-leakage, low volatility, flammability, and dendrite resistance[33].

In the pursuit of developing lithium metal batteries, researchers have endeavored to improve the mechanical properties of SPEs to hinder the formation of lithium dendrites. A theoretical prediction suggests that the growth of lithium dendrites can be prevented by ensuring that the shear modulus (G) of

the separator/electrolyte is twice that of lithium metal ($G > 2G_{Li}$, or $G > 6G_{Pa}$ at room temperature)[26]. Recently, a photopolymerization technique was employed to create an interpenetrating network of poly(ether-acrylate) SPE, which combines impressive mechanical strength (≈12 G_{Pa}) and high ionic conductivity (2.2×10^{-1} mS·cm^{-1} at room temperature), effectively preventing dendrite growth and facilitating Li-ion migration for efficient lithium metal plating/stripping. Nevertheless, Tikekar *et al.* disputed the necessity of the $G > 2G_{Li}$ criterion to inhibit lithium dendrite growth[34]. They developed an SPE utilizing polyethylene (PE) cross-linked with PEO segments[12]. The incorporation of PE backbones decreased the crystallinity of PEO, thus enhancing ionic conductivity. The addition of polyethylene glycol (PEG) allowed for tuning of the SPE, resulting in a plasticized cross-linked polymer with a high ionic conductivity of 2.0×10^{-1} mS·cm^{-1} at 25 °C. The dendrite-resisting properties of the SPE were demonstrated through testing with a charge passed through the cell at various current densities. The cross-linked SPEs increase the lifetime of the Li cells by over an order of magnitude that of PEO, which indicates their exceptional dendrite-resisting capability despite their modest shear moduli.

Pan *et al.* recently introduced a new cross-linked SPE that utilized polyhedral oligomeric silsesquioxane (POSS) and PEG to address lithium dendrite formation [Figure 6A and B][35]. The researchers found that POSS particles provided the necessary mechanical strength for the cross-linked polymer electrolyte, while PEG chains facilitated ion conduction. The mechanical properties of the cross-linked SPEs were measured via dynamic mechanical analysis (DMA) using a three-point bending mode [Figure 6C]. By varying the molar ratio of POSS to PEG and the molecular weight of PEG in POSS-nPEGm, the researchers can optimize the shear modulus and ionic conductivity of the polymer electrolyte. Results showed the ionic conductivity increased with the POSS/PEG ratio [Figure 6D]. At 105 °C, the POSS-4PEG2K electrolyte had a high conductivity of > 1 mS·cm^{-1} and maintained a shear modulus of 33.6 MPa. While the moduli of the POSS-nPEGm electrolytes did not meet the modulus criterion to mechanically prevent lithium dendrite growth, the cross-linked polymer electrolytes were effective in blocking lithium dendrites and improving cell life. The symmetric cell using POSS-4PEG2K [Figure 6E] was tested at different current densities. The cell was still stable after 2,600 h of cycling at 0.3 mA·cm^{-2} for POSS-4PEG2K [Figure 6F]. These findings demonstrate the promising potential of the cross-linked polymer electroly

The inorganic solid electrolyte boasts exceptional ionic conductivity and mechanical properties. However, its high brittleness, complex processing, and elevated interfacial impedance impede its practical applicability. In contrast, the polymer electrolyte offers superior flexibility and machinability, enabling its seamless connection with lithium metal. Nonetheless, the ionic conductivity of the polymer electrolyte is suboptimal, which dampens its practicability. To exploit the benefits of both electrolyte types, researchers have devised a novel polymer-inorganic composite electrolyte. The interaction between inorganic particles and polymer electrolytes can mitigate polymer crystallization and enhance ionic conductivity. The incorporation of polymers likewise reduces the interfacial resistance between lithium metal and the solid electrolyte. Zhao *et al.* probed into the ternary sulfide $Li_{10}GeP_2S_{12}$ (LGPS) and a PEO lithium salt system to assemble a composite electrolyte with high Li^+ conductivity (1.18×10^{-2} mS·cm^{-1})[36]. The effect of the solid plasticizer succinonitrile (SN) on the ionic conductivity of PEO electrolytes has been widely examined, culminating in the successful preparation of a new SPE (PEO_{18}-LiTFSi-1%LGPS-10%SN) via conventional solution casting. Its maximum ionic conductivity reaches 9.1×10^{-2} mS·cm^{-1} at 25 °C, 15 times larger than that of PEO-LiTFSI[37].

The Li/PEO_{18}-LITFSi-1%LGPS-10%SN/$LiFePO_4$ battery demonstrates impressive cycling and capacity results at 40 °C. The battery reaches a maximum discharge capacity of 138.4 mAh·g^{-1} at 0.5 °C, and the capacity retention rate is nearly 90% even after 100 cycles. The newly-developed SPE effectively inhibits

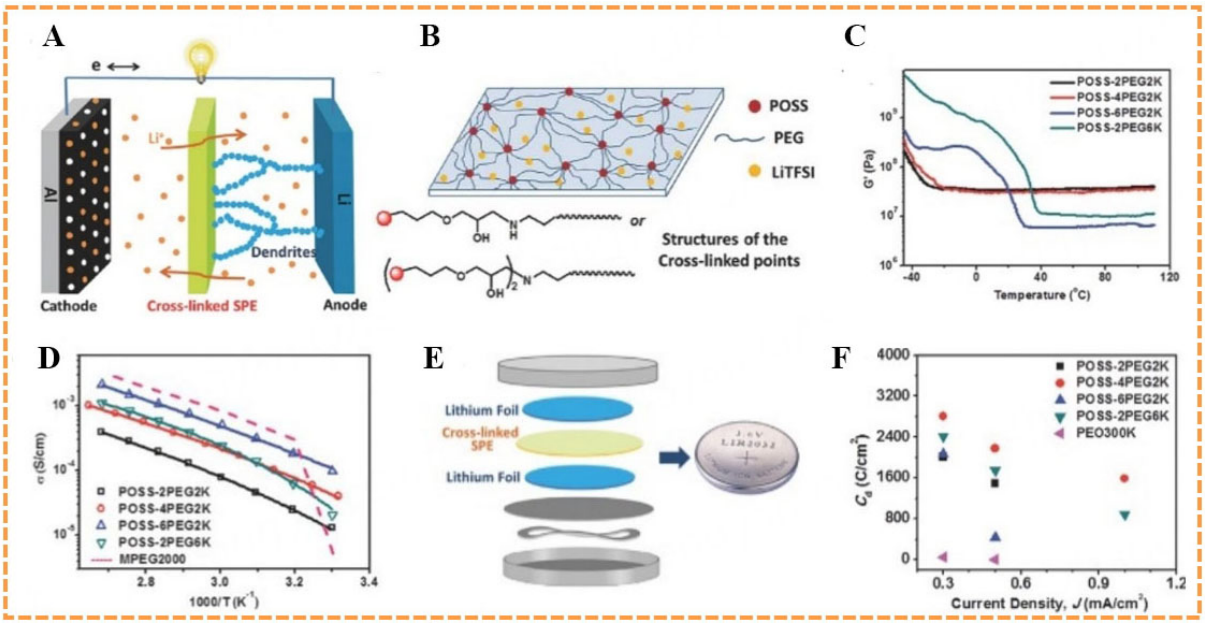

Figure 6. (A) Schematic illustration of LMB with a cross-linked POSS-PEO SPE as the separator to block the growth of lithium dendrites. (B) Schematic presentation of the cross-linked POSS-PEG hybrid polymer electrolyte on Li-metal anode to block Li dendrites; (C) The storage modulus G′ and (D) ionic conductivity of the POSS-PEO solid polymer electrolytes as functions of temperature; (E) Configuration of the lithium symmetric cell; (F) Charge passing the lithium symmetric cell (Cd) in the galvanostatic cycling tests at different current densities[35]. Copyright 2015, WILEY.

dendrite growth, which contributes to the outstanding electrochemical performance of the battery. The research group incorporated $Li_{1.5}Al_{0.5}Ge_{1.5}(PO_4)_3$(LAGP) active particles of varying sizes and ratios into PEO to produce various composite electrolytes (PEO-LAGP)[38]. It was found the electrolyte with the smallest particle size had the highest conductivity of 0.676 mS·cm^{-1} at 60 °C. By using composite electrolytes (PEO-20%LAGP-l), the researchers assembled Li/PEO-20%LAGP-l/$LiFePO_4$ cells, which achieved a capacity of 100 mAh·g^{-1} with a capacity retention rate of nearly 90% after 50 weeks of cycling at 1 and 60 °C. Notably, the capacity retention rate for Li/PEO/$LiFePO_4$ batteries under the same conditions is only 44% after 50 cycles. The addition of LAGP-I particles to PEO significantly improves the interface stability and compatibility, thereby optimizing the battery performance. Furthermore, the researchers designed a novel composite electrolyte with layered structures to address the different needs of positive and negative interfaces. The Goodenough Research Group developed a polymer/ceramic/ polymer sandwich structure composite electrolyte (PCPSE)[39]. In this design, the inorganic layer blocks the transportation of lithium salt anions, reduces the influence of space charge on the lithium and electrolyte interface, and thus relieves the interface impedance. The Li/PCPSE/$LiFePO_4$ battery demonstrated excellent performance and achieved a specific capacity of ~100 m·Ah·g^{-1} after 640 cycles of charging and discharging at a current density of 0.51 mA·cm^{-2}.

The primary objective of optimizing polymer electrolytes, as mentioned above, lies in elevating their mechanical hardness and enhancing their electrical conductivity, which effectively prevents dendritic growth, assures lithium battery safety, and concurrently maximizes the CE. In addition to the polymer electrolyte modification strategies mentioned previously, hybrid electrolytes comprising polymers and nanomaterials offer significant potential for electrolyte optimization. The rapid development of nanotechnology presents endless opportunities for enhancing electrolytes, significantly improving ion flow within the electrolyte. Detailed investigations of polymer-nanomaterial electrolytes are discussed below.

Polymer-nanomaterial composite electrolytes

In general, the composite electrolytes of polymers and nanomaterials significantly enhance the safety and performance of metal lithium batteries. Firstly, utilizing composite electrolytes can significantly improve the mechanical strength and tensile resistance of the electrolyte, affording it higher stability and reliability. Compared with traditional electrolytes, polymer-nanomaterial composite electrolytes effectively reduce safety issues, such as thermal runaway and electrolyte leakage. Secondly, owing to their large specific surface area and unique conductivity, nanomaterials, when combined with polymer electrolytes, enable an enhanced ion transmission in the electrolyte, improving the electrochemical performance and cycle stability of the battery and prolonging its lifespan. Moreover, polymer-nanomaterial composite electrolytes can delay the formation and growth of lithium dendrites, thereby reducing the risk of short circuits within the battery. Several types of polymer-nanomaterial composite electrolytes will be specifically introduced in the following section.

The integration of nanofillers into polymer electrolytes can yield a higher elastic modulus and an expanded electrochemical stability window. Lin *et al.* reported a high-ionic-conductivity PEO electrolyte fortified with monodispersed ultrafine SiO_2 nanospheres[40]. The incorporation of nanoparticles corresponded with an impressive 1-2 orders of magnitude increase in ionic conductivity in comparison to the pure polymer matrix, which was attributed to the structural rearrangement of the interface around the nanoparticles. Polymers and active fillers share a common component, which elicits a driving force and balances the lithium chemical potential between the two phases[41].

The incorporation of active nanowires or nanofiber networks into polymer matrices can significantly enhance ionic conductivity by offering long ion transport pathways in the polymer matrix [Figure 7A]. Liu *et al.* recently demonstrated the potential of one-dimensional $Li_{0.33}La_{0.55}7TiO_3$ nanowires as excellent fillers in composite electrolytes, resulting in enhanced ion conduction[42]. When the $Li_{0.33}La_{0.55}7TiO_3$ nanowire content was at 15 wt.%, the ionic conductivity of the electrolyte reached 0.24 mS·cm^{-1} at ambient temperature. The increase in ionic conductivity was due to the strong complexation between ClO_4^- and the acidic groups on $Li_{0.33}La_{0.55}7TiO_3$, resulting in the dissociation of $LiClO_4$ and the generation of a fast Li-ion diffusion channel [Figure 7B]. Similarly, the utilization of $Y_2O_3^-$ and ZrO_2 nanowires with positive oxygen vacancies on their surface can interact with salt anions, releasing Li-ions and resulting in the formation of a continuous fast conduction path[43]. This interaction improves the ionic conductivity of composite polymer electrolytes, offering a greater advantage than a single nanoparticle [Figure 7B].

Fu *et al.* have explored the potential benefits of using 3D garnet-type $Li_{6.4}La_3Zr_2Al_{0.2}O_{12}$ (LLZO) nanofiber networks to enhance the ionic conductivity of dry polymer electrolytes[44]. The LLZO nanofiber network acts as an effective medium for the continuous transportation of Li-ions in the electrolyte system [Figure 7C]. Figure 7D illustrates the preparation process of a fiber-reinforced polymer composite electrolyte, which involves the utilization of electrospinning technology. Initially, a combination of garnet LLZO salt and the sacrificial polymer was spun into nanofiber membranes and subsequently sintered at 800 °C in the air to form a garnet ceramic nanofiber network. SEM images reveal that these garnet nanofibers possess strong interconnectivity [Figure 7E] and have a membrane thickness ranging from 40-50 microns [Figure 7F].

Solid electrolytes based on garnet nanofibers exhibit high thermal stability and mechanical strength, thereby mitigating the safety hazards (e.g., battery short circuits) that may arise from polymer electrolyte softening or liquefaction at elevated temperatures. Notably, the ionic conductivity of garnet nanofiber solid electrolytes is 0.25 mS·cm^{-1}, which shows high electrochemical stability even under high current densities of up to 0.5 mA·cm^{-2}[44]. Enhancing ion conduction remains a crucial research direction in resolving lithium

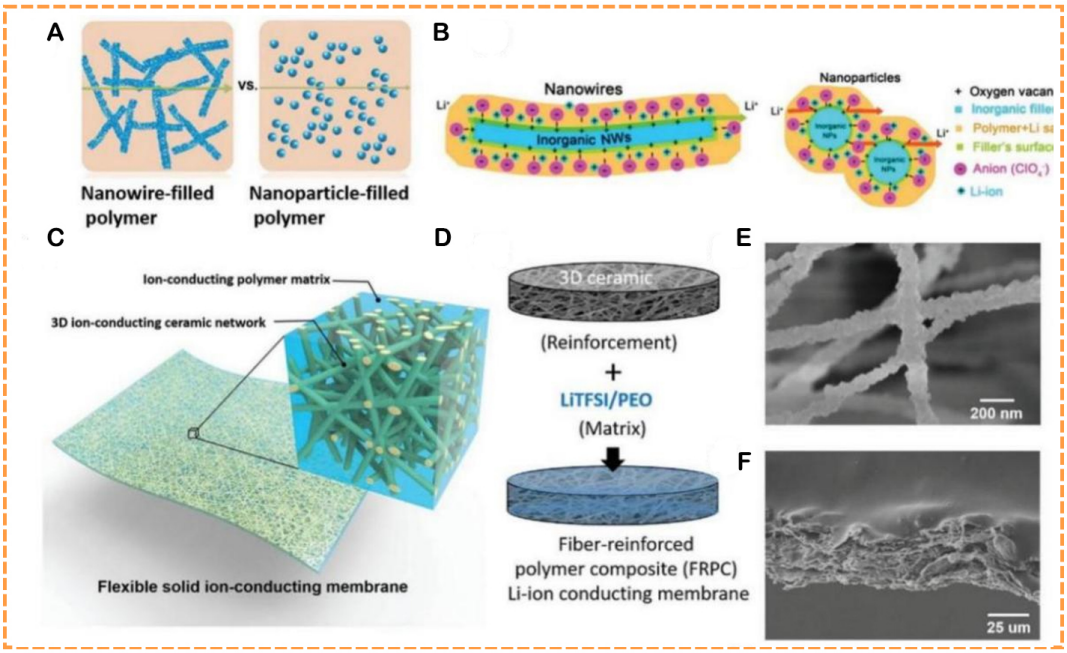

Figure 7. Composite electrolytes using inorganic fillers and SPEs. (A) Schematic of nanowire and nanoparticle fillers in the polymer matrix[42]. Copyright 2015, American Chemical Society; (B) Mechanism of ion transport in nanowire or nanoparticle-filled polymer electrolytes[43]. Copyright 2016, American Chemical Society; (C) Schematic of nanofiber network in the polymer electrolyte; (D) Schematic of preparation of fiber-reinforced polymer composite electrolyte; (E) SEM images of garnet nanofibers and (F) cross-section of the electrolyte composites[44]. Copyright 2017, WILEY. SEM: scanning electron microscopy. SPEs: solid polymer electrolytes.

battery issues. The integration of liquid and solid electrolytes, known as "liquid-solid hybrid electrolytes", has demonstrated the potential to improve ionic conductivity by filling the gap between the solid electrolyte and the electrode.

Liquid-solid hybrid electrolytes

Liquid-solid hybrid electrolytes possess remarkable transport capability, chemical stability, and safety. In the context of metal lithium batteries, this type of electrolyte shows great promise as a potential substitute for traditional electrolytes. In terms of transport capability, liquid-solid hybrid electrolytes offer a more uniform distribution compared to their conventional counterparts, which allows for efficient transfer of Li-ions within the electrolyte. This high-performance transport capability enhances the CE, simultaneously reducing the need for cooling measures and minimizing the risk of thermal runaway. Firstly, liquid-solid hybrid electrolytes contain a greater proportion of flowable media that can maintain excellent flowability even under high-temperature conditions. Secondly, due to the higher concentration of solvents and additives present within the electrolyte system, liquid-solid hybrid electrolytes are better equipped to curtail adverse phenomena, such as lithium dendrite growth or precipitates. Additionally, these electrolytes can effectively reduce the production of gas within the battery, further enhancing the overall safety performance of these batteries, particularly in extreme operating environments characterized by prolonged usage, rapid charge-discharge cycles, or high/low-temperature conditions. The subsequent portion of this exposition shall explicate in meticulous detail several distinct breeds of liquid-solid hybrid electrolytes.

Researchers have extensively studied the structural composition and compatibility of battery interfaces. Among binary liquid-solid electrolyte hybrids, LAGP, $Li_{1.3}Ti_{1.7}Al_{0.3}(PO_4)_3$ (LATP), and lithium super-ionic conductor (LISICON) are commonly used as electrolytes. Hagen *et al.* employed a polymer interlayer that

was saturated with liquid organic solvents as interlayers to optimize the contact between electrodes and solid electrolytes[45]. Additionally, Wang *et al.* developed Li-S cells that utilized $Li_{1.5}Al_{0.5}Ge_{1.5}(PO_4)_3$ as a diaphragm and conventional Li-S electrolyte (LiTFSI in DME/DOL) was filled in the space between solid electrolyte and electrodes[46]. Figure 8A provides a visualization of this battery configuration. Later, Wang *et al.* further extended these advancements by creating a hybrid battery founded on a LISICON-type $Li_{1+x+y}Al_xTi_{2-x}Si_yP_{3-y}O_{12}$ (LATP) solid electrolyte [Figure 8B][47]. Moreover, Yu *et al.* constructed a hybrid battery using a LISICON-type $Li_{1.3}Al_{0.3}Ti_{1.7}(PO_4)_3$ electrolyte, with the dissolved Li_2S_6 catholyte solution acting as a cathode [Figure 8D][48]. The research endeavors undertaken within this area of study provide compelling evidence that indicates a significant improvement in both the CE and capacity of Li-S batteries. However, there is still a lack of thorough understanding regarding interface stability between solid electrolytes and liquid organic electrolytes.

In the realm of lithium battery research, distinguished scholars Busche *et al.* recently investigated the interface between liquid electrolytes and solid electrolytes and revealed the presence of a resistive solid-liquid electrolyte interface (SLEI) at the boundary. Figure 8C delineates a comprehensive schematic diagram of ion transport and resistance contribution at the solid-liquid phase boundary within the battery[49]. The movement of ions across this boundary makes a noteworthy contribution to the total impedance. At the junction between solid and liquid electrolytes, the mechanism underlying ion conduction will shift from the solvation ion diffusion in liquid electrolytes to the hopping mechanism in solid electrolytes. Furthermore, investigations confirm that SLEI encompasses various decomposition products, including inorganic compounds, organic compounds, and polymer compounds. As the thickness of SLEI increases to its maximum, its consequent resistance contribution will eventually reach a threshold. Impedance-wise, the large impedance engendered by the electrolyte-electrode gap must be taken into account, thus making interface engineering an essential consideration.

INTERFACE ENGINEERING

The application of interface engineering in metal lithium batteries not only enhances their safety but also improves CEs, which propels the continuous innovation and development of this technology. Firstly, oxidation reactions and metal lithium formation can be effectively reduced by optimizing the electrode-electrolyte interface structure, thereby significantly decreasing the risk of thermal runaway and fire and explosion within the battery. Additionally, through a thoughtful interface design, such as the addition of surfactants and functionalized molecules, the hydrophilicity of the electrode surface can be improved, which suppresses foam generation within the liquid electrolyte of lithium-ion batteries, thus enhancing both battery charging speed and cycle life. Secondly, interface engineering can significantly improve the CE of metal lithium batteries. For traditional liquid electrolyte systems, the adverse interface reaction between the electrode and the electrolyte often leads to a decline in battery performance and loss, severely limiting the practical applications of metal lithium batteries. However, reasonable interface regulation, using techniques such as introducing polymer nanocomposites, biomaterials, and ionic liquids, can drastically enhance the conductivity and ion transport properties of the battery, which results in remarkable improvements in its CE and cycle life. This article provides a specific introduction to the technology of interface engineering.

SSE surface coating modification

Tsai *et al.* introduced the Au layer on the surface of $Li_7La_3Zr_2O_{12}$ (LLZO) and achieved good results, improving the Li/SSE interface contact[50]. The interfacial resistance was reduced, and no lithium dendrite formation was evident after long-time cycling. Inspired by the unique H^+/Li^+ exchange reaction of garnet-type LLZO, Cai *et al.* directly dropped an $AgNO_3$ aqueous solution onto $Li_{6.4}La_3Zr_{1.4}Ta_{0.6}O_{12}$ (LLZTO) surfaces to construct a lithium-philic layer[51]. This layer swiftly generates a uniformly dispersed layer of Ag

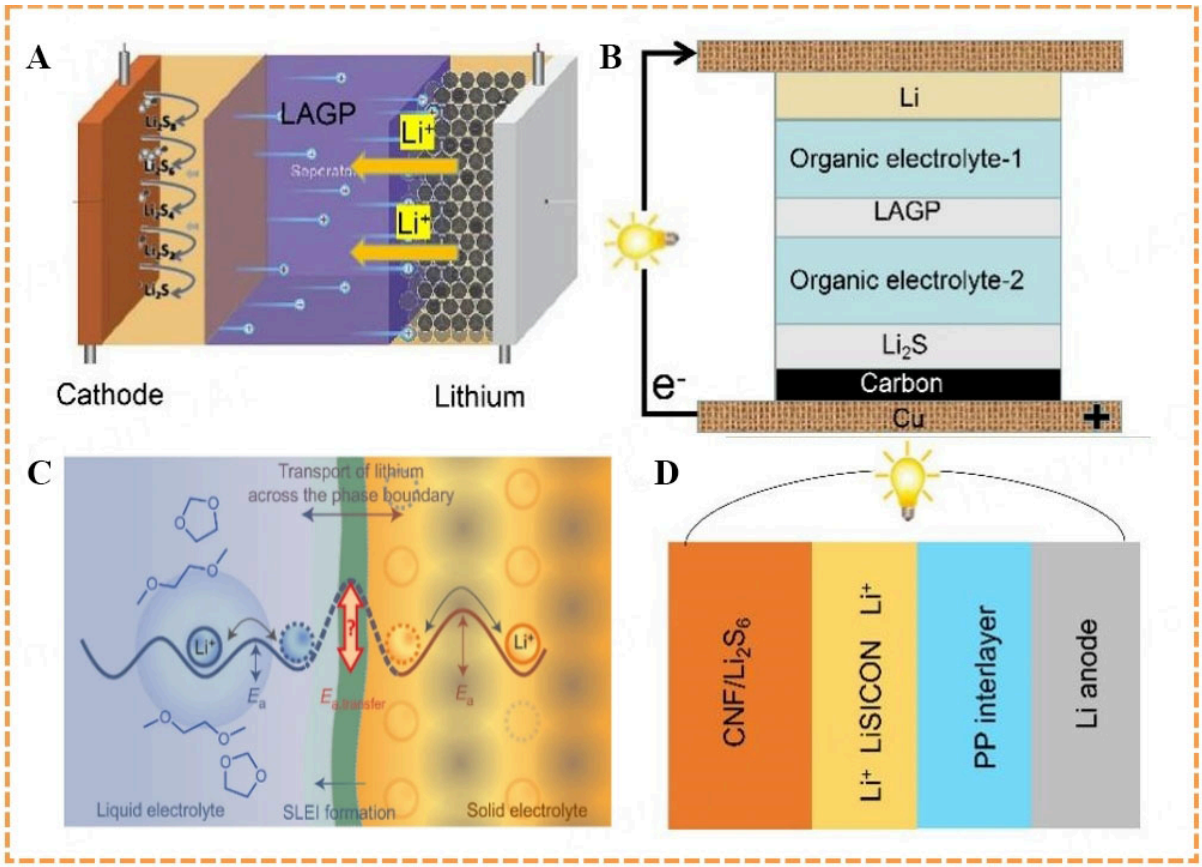

Figure 8. Liquid-solid hybrid electrolytes for Li-metal batteries. Schematics of (A) a hybrid Li-S cell using LAGP solid electrolyte, (B) a hybrid Li-Li_2S cell using LISICON-type LATP solid electrolyte, (C) liquid electrolyte and solid electrolyte[49], Copyright 2016, Macmillan Publishers Limited. (D) a hybrid Li-Li_2S_6 cell using LISICON-type LATP solid electrolyte.

nanoparticles, which subsequently react with molten Li to form Li-Ag alloy. Consequently, interfacial wettability between Li and LLZTO is considerably enhanced, with interfacial resistance reduced to about 4.5 $\Omega \cdot cm^{-2}$. The modified LLZTO was used to assemble a fully solid state. The Li/LLZTO/$LiFePO_4$ cell was cycled at 60 °C for 200 cycles. The cell has good cycling stability and effectively inhibits dendrite growth[52].

Huo *et al.* etched dense LLZTO ceramic sheets in hydrochloric acid for 1 h before fabricating 30 μm 3D-porous LLZTO (3D-LLZTO)[30]. Three different interfaces (unmodified Li/LLZTO, lithium-philic Li/LLZTO@ ZnO(zinc oxide), and Li/3D-LLZTO@ZnO) are constructed, and their deposition behaviors are displayed in Figure 9A-C. Different from conventional coating techniques, this method involves pretreatment of the SSE prior to coating and the construction of a 3D porous surface through acid-etching technology. The 3D-LLZTO@ZnO interface sufficiently reduces local current density and volume fluctuations, thereby effectively curbing dendritic growth. Assembled Li/3D-LLZTO@ZnO/Li symmetric batteries demonstrate a stable cycle lifespan exceeding 600 h at a current density of 0.5 $mA \cdot cm^{-2}$. However, lithium dendrites are clearly visible in both unmodified Li/LLZTO and Li/LLZTO@ZnO lithium symmetric batteries. Sheng *et al.* added Li_2S additive to modify the PEO-LiTFSI interface in developing PEO-LiTFSI-Li_2S solid electrolyte[53]. Modified interface impedance was reduced from 557 to 374 $\Omega \cdot cm^{-2}$. Cryogenic transmission electron microscopy (Cryo-TEM) and molecular dynamics simulations reveal that Li_2S accelerates the decomposition of LiTFSI by constructing *in-situ* interfacial layers rich in highly conductive LiF. The generated LiF effectively inhibits the fracture of C-O in PEO chains and stabilizes the

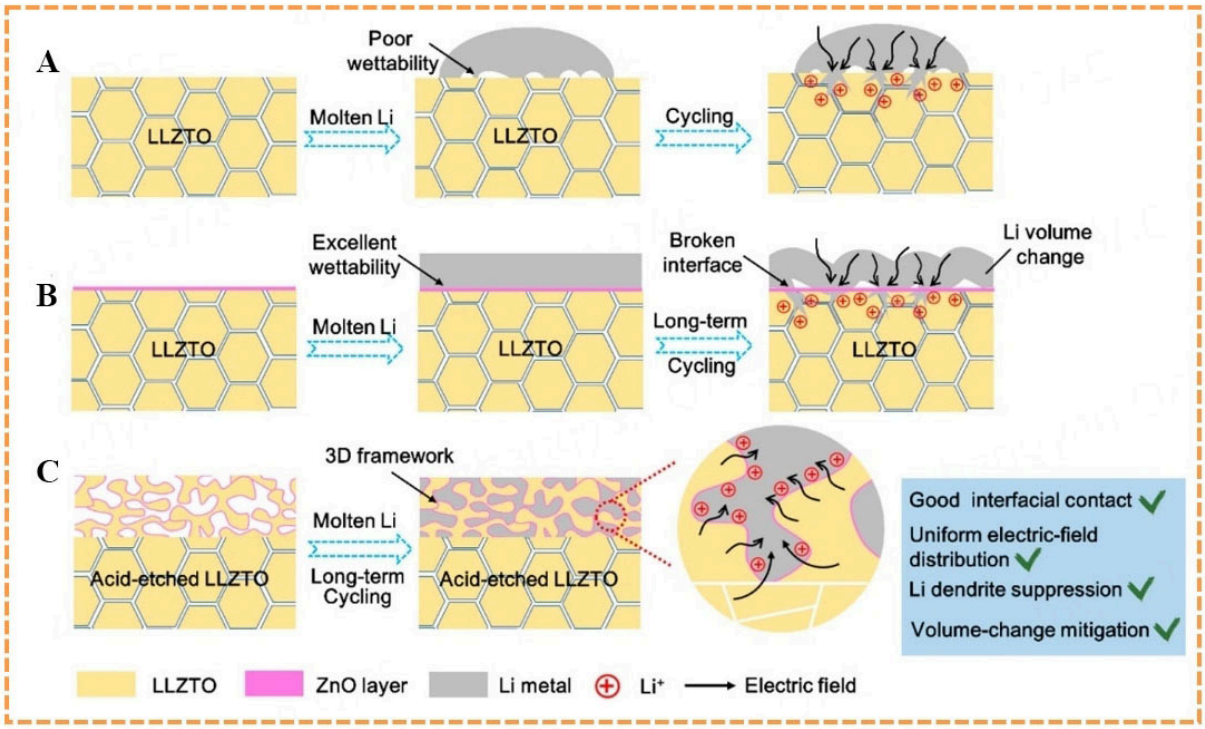

Figure 9. Three different interfacial behaviors of lithium deposition: (A) LLZTO/Li interface; (B) LLZTO@ZnO/Li interface; (C) 3D-LLZTO@ZnO/Li interface[30]. Copyright 2020, American Chemical Society.

Li/PEO interface during cycling. The Li/PEO-LiTFSI-Li_2S/$LiFePO_4$ battery exhibits a specific capacity of 140 mAh·g^{-1} with a CE of 99% at 50 °C and 0.5 C, retaining 85% capacity after 1,000 cycles, significantly better than PEO-LiTFSI batteries (77%, 150 cycles). Table 1 briefly summarizes the functions and mechanisms of the various electrolytes.

The oxide-garnet type SSE, $Li_7La_3Zr_2O_{12}$, exhibits exceptional ionic conductivity, making it an auspicious candidate for solid lithium metal batteries. Despite intensive investigations to enhance chemical stability and ionic conductivity, the poor wettability between lithium metal and garnet electrolyte still engenders many microporous structures and microscopic gaps at the interface[Figure 10A][61]. High interfacial impedance impedes the further development of solid lithium metal batteries; the introduction of an alumina coating can reduce the interfacial impedance by forming a Li-Al-O layer with Li-ion conductivity and electronically insulating properties[61]. The nanoscaled alumina coating ensures optimal wettability and intimate surface contact. In the absence of the ALD coating, a vast physical gap is clearly delineated [Figure 10B], leading directly to interfacial resistance up to 10^3 Ω·cm^{-2}. In contrast, with the presence of the ALD-Al_2O_3 coating, the reaction of Al_2O_3 with molten Li provides the driving force for mutual contact, leading to a marked reduction in total impedance. The interfacial resistance decreases from 1,710 to 34 Ω·cm^{-2} with the addition of the Al_2O_3 layer [Figure 10C]. Moreover, the Li-symmetric garnet cell containing Al_2O_3 manifests a stable potential of about 13 mV at a current density of 0.1 mA·cm^{-2} [Figure 10D]. Conversely, the Li-symmetric garnet cell lacking Al_2O_3 demonstrates a noisy potential. The successful assembly of a battery comprising Li/Al_2O_3 garnet electrolyte and $Li_2FeMn_3O_8$ cathode that powers a light-emitting diode (LED) highlights this potential. Further advancements in SSE engineering and interface modification will undoubtedly pave the way for more stable and efficient lithium metal batteries.

Table 1. Electrolyte additives and functions

Additives	Mechanism	Function
Li_2S[53]	Accelerating the decomposition of LiTFSI	Constructing a stable interface rich in high-conduction LiF
CO_2[54]	Forming Li_2CO_3 protective layer	Stabilizing the interface
HF[55]	Forming LiF-Li_2O layer	Stabilizing Li deposition
Inert additives[56]	Reducing cell impedance	Accumulation at the interface to form a film
Metal ions (Na^+, Mg^{2+})[57]	Forming superficial thin layers of alloys with Li	Suppressing the dendrite formation and improving CE
2-Methylfuran[58]	Ring-opening polymerization at the Li surface to form a film	Improving CE and reducing impedance
Fluoroethylene carbonate (FEC)[59]	Producing a LiF-rich surface film with a uniform structure	Improving CE and suppressing dendrite formation
Vinylene carbonate[60]	Ring-opening polymerization at the Li surface to form a film	Stabilizing the interface

CE: Coulombic efficiency; FEC: fluoroethylene carbonate.

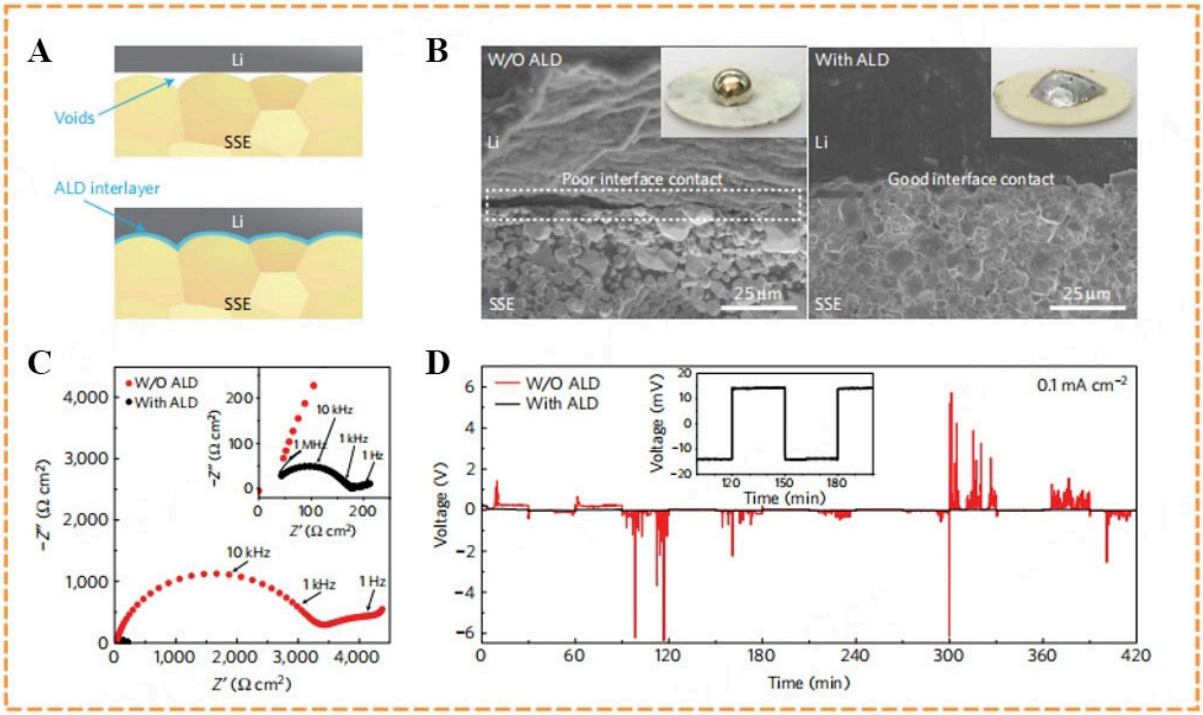

Figure 10. Interface of garnet SSE and Li-metal anode. (A) Schematic of the interface between of garnet surface and metallic Li; (B) SEM images of the garnet solid electrolyte/Li-metal interface. Insets are photos of a drop of molten on a garnet disk; (C) EIS profiles of the symmetric Li/garnet cells with and without ALD coating. Inset shows the enlarged impedance curve of the ALD-treated garnet cell; (D) DC cycling of Li/garnet symmetric cells at a current density of 0.1 mA·cm^{-2}. The inset is the magnified curve of the ALD-garnet cell[61]. Copyright 2017 Macmillan Publishers Limited. ALD: Atomic layer deposition; EIS: electrochemical impedance spectroscopy; SEM: scanning electron microscopy; SSE:solid-state electrolyte.

SSE porous optimization

Constructing an engineered interface (e.g., active material embedded in a porous structure) is another means of reducing interfacial resistance between the electrode and solid electrolyte[62]. Figure 11A compares planar interfaces with porous interfaces. Sacrificial organic templates are added onto high-density solid electrolyte micelles, which are promptly removed by sintering for the creation of the porous interface. A

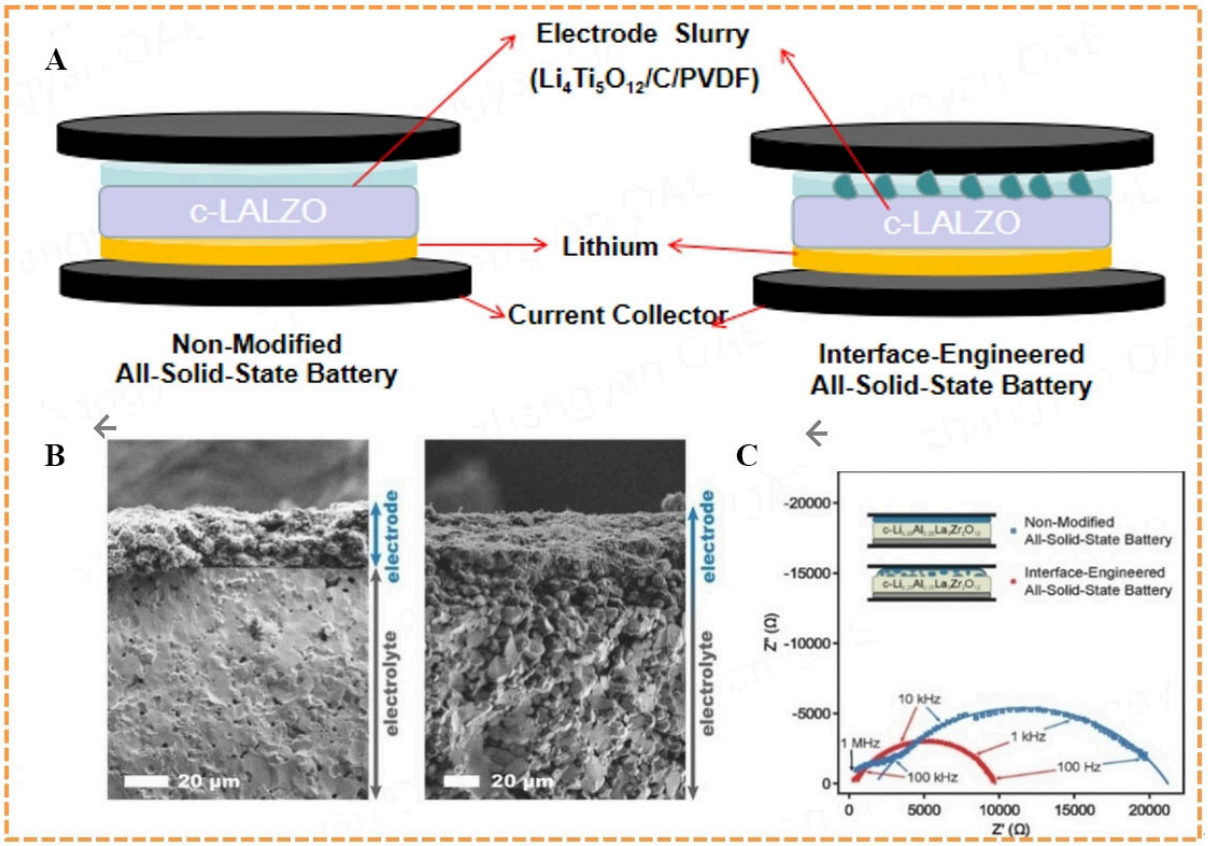

Figure 11. Nanoengineering on SSE for interface contact. (A) Schematic of non-modified or interface-engineered solid-state battery; (B) SEM images of cross-sectional interfaces of the electrolyte and electrode for non-modified or interface-engineered pellets; (C) Nyquist plots of non-modified or interface-engineered batteries[62]. Copyright 2016, WILEY. SEM: scanning electron microscopy.

slurry consisting of $Li_4Ti_5O_{12}$, conductive carbon, and the polymer is cast on a planar or porous structure [Figure 11A]. Cross-sectional SEM images of both interfaces are compared [Figure 10B]. In the non-modified cell, a distinct poor interface occurs, leading to extremely high interfacial impedance [Figure 11C]. However, after interface engineering modification, the electrode layer is tightly embedded in the porous solid electrolyte layer, with almost no gap or splitting between electrolyte and electrode. To make further strides toward improving the efficiency and efficacy of SSEs, it is recommended that more attention shall be devoted to the development of interface-engineered structures as well as the construction of sturdier SSE frameworks. Significant progress will be made in lithium batteries by optimizing the contact area between electrodes and SSEs via these techniques.

Lithium anode surface coating modification

In recent years, researchers have explored the application of Au, Si, and ZnO on Li surfaces. Tsai *et al.* utilized a thin Au buffer layer to enhance contact and minimize lithium dendrite formation [Figure 12A][50]. The Au buffer layer significantly reduced the total resistance of the Li-symmetric solid electrolyte cell from 3,000 to 380 $\Omega \cdot cm^{-2}$. At room temperature, Au and Li combine to create a unique contact with the solid electrolyte, enabling the redistribution of Li dissolution and deposition. After the groundbreaking research, subsequent studies have delved into the application of Si and ZnO. More specifically, an ultrathin layer (about 10 nm) of amorphous Si was conformally coated onto a garnet electrolyte through chemical vapor deposition[63]. ZnO has been identified as yet another active material that can react with molten Li at the interface, eventually leading to the formation of a Li-Zn alloy [Figure 12B][64]. The coating layer of ZnO can

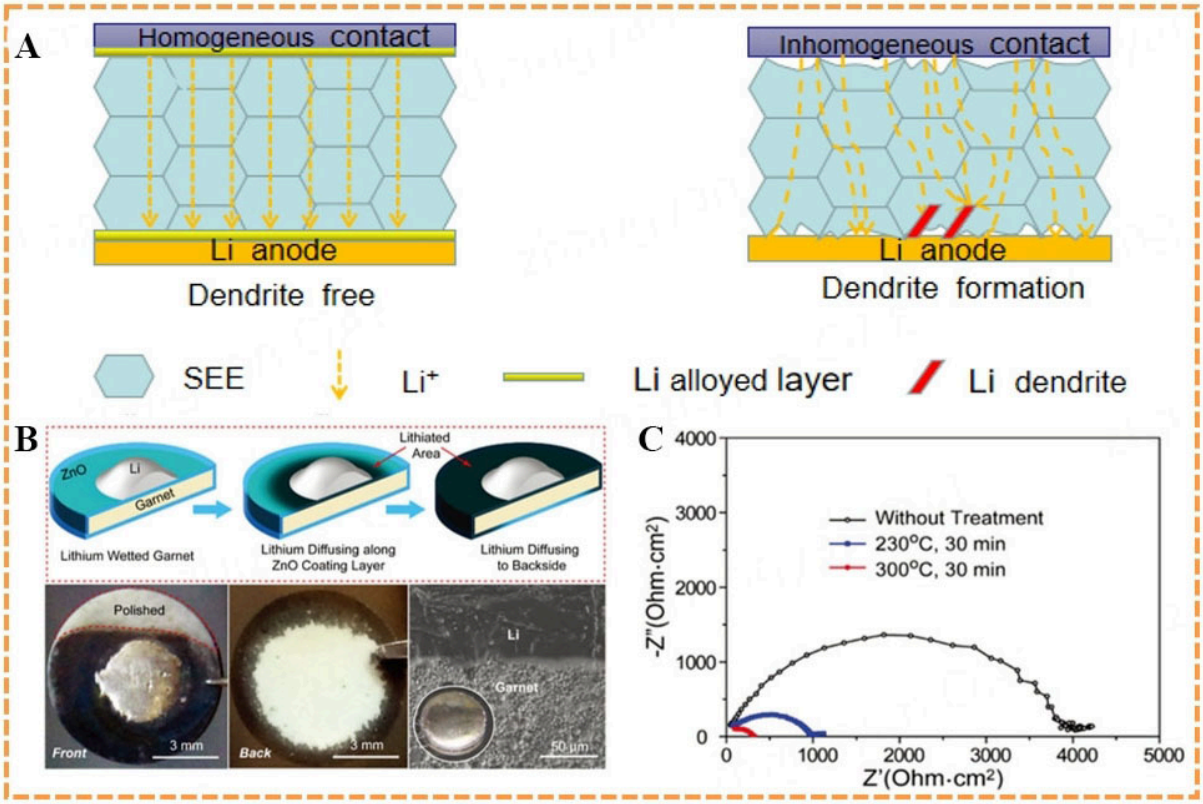

Figure 12. Li-SSE interface wettability improvement via Li alloys. (A) Garnet/Li interface with an Au buffer layer to improve its interfacial contact; (B) Schematics, digital photos, and SEM images showing the wettability of garnet-Li interface with a ZnO coating layer; (C) EIS of the Li symmetric cells with or without ZnO[64]. Copyright 2016, American Chemical Society. EIS: electrochemical impedance spectroscopy; Li: Lithium; SEM: scanning electron microscopy. EIS: electrochemical impedance spectroscopy; SEM: scanning electron microscopy.

facilitate high-speed diffusion of molten Li, thereby ensuring the optimal contact between Li and the garnet solid electrolyte while effectively suppressing interfacial resistance [Figure 12C].

Interface engineering technology has demonstrated a significant improvement in battery performance. Additionally, optimizing the physical properties of the electrodes presents a viable strategy for enhancing battery efficiency. The next section of this review will delve into a common electrode modification technique - designing an electrode framework.

ELECTRODE FRAMEWORK DESIGN

Creating a 3D framework structure for electrodes is an effective solution to enhance the safety and CE of metal lithium batteries[65]. With continued development and improvement, this technology has the potential to become a critical component in the future of metal lithium batteries, with more widespread applications. Firstly, the use of a 3D framework structure for electrodes can significantly reduce the risk of thermal runaway within the battery. The formation of abundant metal lithium on the surface of electrode materials accompanied by substantial volume changes during discharge often leads to extreme situations, such as surface melting or short circuits. Therefore, transforming traditional planar electrodes into electrodes with a 3D framework structure can mitigate these problems to some extent. Secondly, the 3D framework structure of electrodes can also enhance the CE of the battery. Compared with traditional battery structures, these electrodes with a 3D framework provide a larger interface area and expose more active material to the

electrolyte, resulting in faster ion transport, lower internal resistance, improved charge-discharge efficiency, and longer cycling lifespan. Furthermore, a 3D framework structure of electrodes can improve the mechanical stability, vibration resistance, and bending resistance of the battery, thereby enhancing its service life and safety. This overview will provide a comprehensive and specific analysis of the 3D framework structure for electrodes.

Researchers are actively engaged in the development of a 3D anode skeleton (or 3D current collector), a promising approach for enhancing battery performance. The 3D frameworks can augment anode-specific surface area to promote uniform distribution of Li-ions on the surface, reducing local current density and thereby mitigating side reactions between the electrode and electrolyte. Common 3D skeletons include porous conductive materials, such as copper foam metal, nickel foam metal, carbon fiber film, and graphene film. Non-conductive frameworks, such as dry wood, polyimide (PI), and glass fibers, also have natural channels that facilitate ion transport. However, their commercial application is impeded by limitations, such as poor mechanical properties and cumbersome preparation[66].

3D framework lithiophilicity optimization

The role of lithiophilicity in achieving uniform Li-ion deposition is of utmost importance. Due to the typically high nucleation barriers of 3D frameworks and poor affinity with Li-ions, it is customary to deposit a lithiophilic transition layer on the surface of the substrate to enhance its lithiophilicity[67,68]. Recently, Wang *et al.* reported a method to modify a collector framework (NRA-CC) based on a 3D carbon cloth with lithiophilic metal-organic framework (MOF) nanorod arrays[69]. The schematic illustration of a synthesis process of the NRA-CC is displayed in Figure 13A. The NRA-CC was immersed in a solution of nitric acid and dimethylimidazolidinone precursor to generate Co-based MOF nanorod arrays *in situ* on the surface of the 3D carbon cloth, which was then carbonized to form a C-N-Co three-phase nanoscale modified layer. This structure can significantly enhance the lithiophilicity of the 3D framework surface.

This study sought to explore the practical feasibility of a Li@NRA-CC hybrid anode by incorporating it into full batteries equipped with high-voltage $LiNi_{0.5}Co_{0.2}Mn_{0.3}O_2$ (NCM) cathodes. The battery operated with the Li@NRA-CC anode delivered outstanding cyclic stability, retaining about 75% of its initial capacity after 200 cycles with minimal voltage hysteresis fluctuations [Figure 13B]. In sharp contrast, the performance of the full battery containing Li foil as an anode degraded drastically within only 60 cycles and exhibited fluctuating CEs, indicating poor electrode-electrolyte interface stability [Figure 13C]. These two different battery configurations displayed analogous trends in rate performance when the current density did not exceed 1 C [Figure 13D and E]. However, upon increasing the rate to 5 C, the capacity of the battery utilizing Li foil decreased rapidly, while the battery oriented as a Li@NRA-CC anode yielded resilient capacity values coupled with relatively stable cyclic stability. Therefore, the application of a 3D porous carbon cloth framework has enhanced the cycling performance of the battery, effectively guiding lithium-ion deposition uniformly on the 3D framework surface and suppressing negative electrode volume expansion and dendrite growth. The pore size of the 3D framework shall also be appropriate, as excessively large or small pores may not be conducive to Li deposition.

Innovative 3D fluid collections

Porous 3D lithium substrates can effectively adjust to volume fluctuations during cycling. This review presents a variety of innovative fluid collections. Among the various substrate materials, carbon-based materials or metal frames are widely utilized as current collectors. These 3D nanostructured conductive substrates offer a network of free electron pathways and ensure full contact with liquid electrolytes, facilitating rapid charge transfer and uniform lithium nucleation. Among the carbon-based host materials, Ji *et al.* reported an inhomogeneous 3D current collector with modified carbon paper to prohibit Li

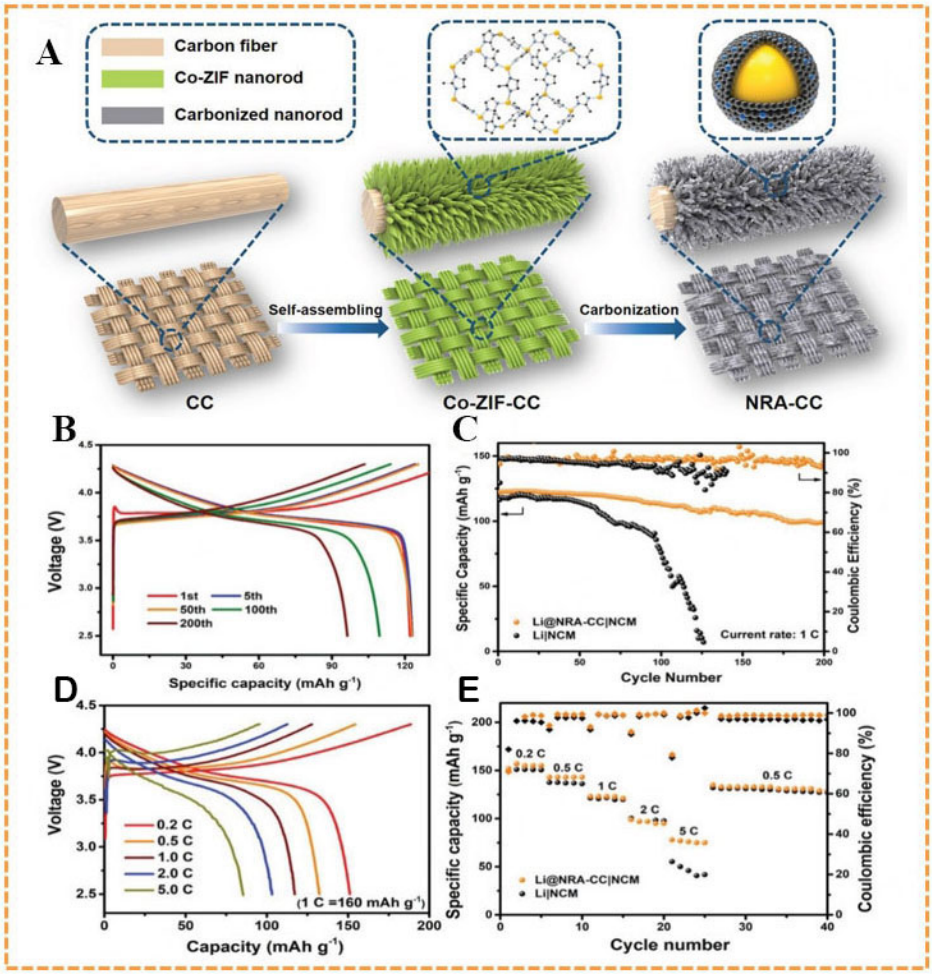

Figure 13. (A) Schematic illustration of the synthesis procedures of NRA-CC; (B) Galvanostatic discharge/charge profiles of the Li@NRA-CC|NCM battery at 1 C (1st-200th cycle); (C) Long-term cycling performance of the Li@NRA-CC|NCM and Li|NCM batteries at 1 C; (D) The charge-discharge curves of Li@NRA-CC|NCM battery at different rates; (E) Rate performance of Li@NRA-CC|NCM and Li|NCM batteries[69]. Copyright 2020, WILEY.

deposition onto the separator. A SiO_2 or SiC insulating layer was applied to the line-of-sight side (facing toward the separator) of the pristine carbon paper [Figure 14B][70]. The spatially heterogeneous insulating property from SiO_2 or SiC coating restricts Li-ions from depositing on the front side of the carbon paper, resulting in a surface dendrite-free Li deposition and inhibition of short circuit even at 4 $mA{\cdot}cm^{-2}$ after a deep Li deposition of 28.8 $C{\cdot}cm^{-2}$[70]. Many other promising carbon hosts that can accommodate lithium metal have been proposed.

Jin *et al.* described a 3D-layered porous carbon material that promotes uniform stripping/plating of lithium metal [Figure 14F][71]. The ZnO@HPC (hierarchical porous carbon) scaffold was synthesized through a precipitation reaction of zinc acetate dihydrate ($Zn(OAc)_2{\cdot}2H_2O$) and lithium hydroxide monohydrate ($LiOH{\cdot}H_2O$) in dilute ethanol solution. The content of ZnO can be easily controlled by varying the amounts of $Zn(OAc)_2{\cdot}2H_2O$ and $LiOH{\cdot}H_2O$. Samples with 5%, 15%, 25%, and 50% ZnO by weight were prepared, and the particle size of ZnO was kept similar for each sample by controlling the concentrations of the $LiOH{\cdot}H_2O$ and $Zn(OAc)_2{\cdot}2H_2O$ solutions. However, differences still existed in the number and distribution of ZnO particles. In comparison to the 15% ZnO@HPC, too little ZnO in the 5% ZnO@HPC induced non-uniform

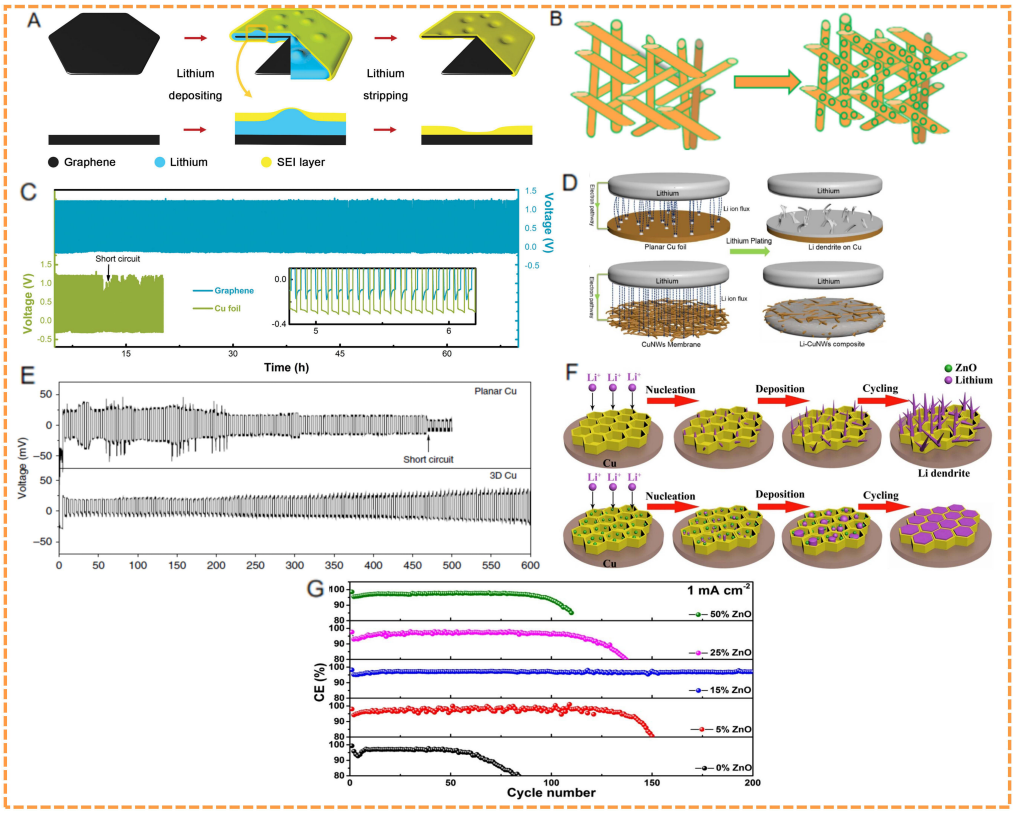

Figure 14. Li-metal anode with a 3D substrate. (A) Schematic illustration of unstacked graphene electrode before (left) and after Li plating (middle) and after stripping (right); (B) Structure illustrations of pristine carbon paper, spatially SiC or SiO_2 coated carbon paper, and Li deposition on this modified carbon paper; (C) Voltage profiles of Li electrodes on the unstacked graphene or Cu foil at 2.0 mA·cm^{-2} with a capacity of 0.1 mAh·cm^{-2} [72]. Copyright 2016, WILEY; (D) Illustration of electrochemical Li plating on planar Cu and 3D Cu[73]. Copyright 2016 WILEY; (E) the corresponding cycling stability of Li on planar Cu and Li in 3D Cu electrodes at 0.2 mA·cm^{-2}[74]. Copyright 2015 Macmillan Publishers Limited; (F) Schematic diagrams for comparison of Li deposition within hierarchical porous carbon scaffold with and without decoration of ZnO nanoparticles; (G) The comparison of the Coulombic efficiency of Li deposition on pristine HPC and various ZnO@HPC[71]. Copyright 2017, Elsevier.

deposition of lithium. Additionally, severe aggregation occurred in both the 25% ZnO particles and the 50% ZnO@HPC samples. Excessive ZnO particles may impair the uniform deposition of Li because they may occupy too much pore space, resulting in excessive discharge products of lithium oxide. Figure 14G compares the CE of Li deposition on different ZnO@HPC samples. Evidently, the CE is correlated with the content of ZnO. Lithium metal up to 131 mAh·cm^{-2} can be confined within ZnO@HPC, achieving acceptable volume expansion, considerable reduction in overpotential, and effective dendrite suppression.

Zhang *et al.* recently presented a remarkable non-stacked graphene framework with nanoscale hexagonal drums that facilitate desirable sites for Li deposition[72]. As illustrated in Figure 14A, the top layer comprises the SEI layer, followed by the deposited lithium metal in the middle and, finally, the graphene framework at the bottom. This innovative anode structure adopts a sandwich-like configuration. The larger specific surface area of nanodrums orchestrates uniform current dispersion and local current density reduction, enabling uniform Li deposition to take place beneath the SEI layer. Li deposition on nanostructured graphite or graphene electrodes manifests better cycling stability. In comparison to planar copper electrodes, the graphene-based anode exhibits enhanced stability over 800 cycles with a negligible hysteresis of 150 mV at 2 mA·cm^{-2} and an excellent capacity of 0.5 mAh·cm^{-2} [Figure 14C].

A simple approach is to increase the surface area of the electrodes to reduce the current density. Along this line, various current collectors, including 3D current collectors with submicron skeletons, 3D porous copper current collectors with vertically aligned microchannels, and independent copper nanowire (CuNW) networks, are used to accommodate volume expansion and inhibit lithium dendrite growth[73]. For planar copper collectors, lithium growth is accelerated in a limited area due to the high local electric field strength [Figure 14D]. In contrast, interconnected CuNWs with a high surface area can significantly reduce the Li-ion flux and thus achieve more uniform Li deposition at the macroscopic scale. In particular, once some dendrites appear, they are confined to the interconnected network, forming lumpy lithium instead of needle-like lithium. Using a stand-alone CuNW network collector, the lithium metal can work stably for 200 cycles, maintaining an average CE of up to ≈98.6%[73]. Yang *et al.* developed a novel 3D copper electrode with submicron holes to optimize lithium metal deposition. Compared with planar copper foil, the battery utilizing 3D copper as an electrode demonstrated excellent cycle stability, lasting for 600 h [Figure 14E][74]. Lu *et al.* discovered that forming 3D porous copper electrodes can effectively strip Zn from Cu-Zn alloys[73]. The pore sizes of 3D porous copper electrodes range from 200 nm to 2 μm, with many protrusions on their inner surfaces providing charge centers and nucleation sites for Li deposition. Self-evaporation of CuNW suspension can synthesize CuNW membranes. After 200 cycles, the cycle efficiency of the 3D copper anode exceeds 97%[74]. The optimized cell performance can be attributed to the significantly reduced local current density resulting from the 3D copper pores, allowing Li deposition to transpire within them and restraining the growth of lithium dendrites.

The carbon nanotube sponge boasts a sizeable specific surface area (300-400 $m^2 \cdot g^{-1}$) and exhibits high porosity (> 99%), making it an ideal 3D host material for lithium metal anodes[75], which is unattainable using traditional planar collectors. Consequently, Zhang *et al.* created a 3D current collector to serve as a host for Li deposition by growing a conformal layer of Al_2O_3 on the carbon nanotube sponge via ALD[76]. The Al_2O_3 layer provides excellent chemical stability and high mechanical strength, providing robust protection to enhance the interface between the 3D electrode and electrolyte. In carbonate electrolytes without additives, the modified electrodes exhibit stable cycling with improved CEs[76].

Molten lithium pre-injected 3D skeleton

The encapsulation of lithium metal within the intricate 3D structure remains a daunting task on account of the exceptional reactivity exhibited by lithium, thereby rendering it technically challenging. Consequently, the current approach utilized for this purpose involves pre-depositing Li on the 3D substrate through electrochemical treatment. Unfortunately, pre-deposition is an arduous and costly procedure.

Chen *et al.* achieved stable lithium metal cycling by designing a novel type of 3D current collector, which uncovered a new mechanism for the deposition/stripping of lithium metal[77]. They combined two mixed-ion-electron conductors (MIECs) and ion-electron-insulated (ELI) materials to stabilize the lithium metal electrochemically, ultimately constructing a 3D tubular lithium metal negative electrode composed of MIEC as the primary channel and ELI for sealing [Figure 15A]. Lithiated carbon tubules with a width of about 100 nm were employed as the MIEC material. The researchers demonstrated the plating and stripping of lithium or sodium inside individual carbon tubules. A solid electrolyte consisting of a PEO-based polymer with a thickness of around 50 μm was utilized in this experiment. On the opposite side of the solid electrolyte, a Li counter-electrode was coated and connected to a scanning tunneling microscope (STM)/transmission electron microscope (TEM) manipulator. The TEM copper grid served as the current collector attached to the carbon tubules on the other end. Notably, the inner diameter of the carbon tubule is around 100 nm, while its walls, with a width of 20 nm, are also nano-porous. *In-situ* TEM showed that lithium metal can advance and contract in a single-crystal form within the MIEC small tube and reversibly deposit/strip on a scale of tens of micrometers, preserving structural integrity within 100 cycles[78]. The Coble creep

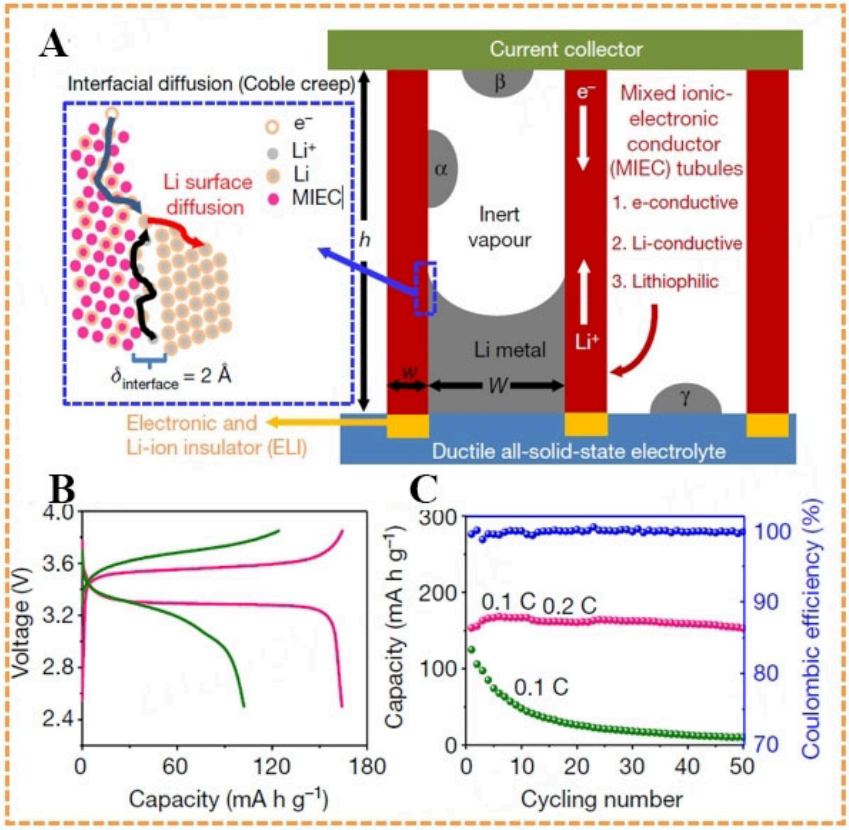

Figure 15. (A) Schematic process of creep-enabled Li deposition/stripping in an MIEC tubular matrix, where Coble creep dominates via interfacial diffusion along the MIEC/Libcc incoherent interface; (B) Charge/discharge profiles at 0.1 C; (C) cycling life of the all-solid-state Li-pre-deposited MIEC/SE/ $LiFePO_4$ batteries. The magenta (capacity) and blue (CE) colors indicate the use of 3D MIEC tubules on Pt foil as a Li host, the discharge capacity of which reaches 164 mA h g^{-1} at 0.1 C and 157 mA·h·g^{-1} at 0.2 C, while the green color indicates the use of 2D carbon-coated Cu foil as a Li host[77]. Copyright 2020, Springer Nature.

mechanism along the MIEC metal lithium interface prevents the formation of dead lithium. Therefore, this structure solves dynamic issues since most deposition/stripping of lithium metal occurs within the electrochemically stable MIEC small tube, thus reducing direct contact between lithium metal and SSEs to produce SEI, ultimately achieving high reversibility of lithium metal negative electrode-SSE interface. This 3D design strategy provides a new approach for constructing high-performance full solid-state lithium metal batteries based on the Coble creep mechanism. MIEC materials shall exhibit good Li-ion and electron conductivity, be absolutely stable to lithium metal electrochemically, and have lithium affinity, which is conducive to pre-lithiation in the battery assembly stage and helps maintain contact between lithium metal and MIEC wall, enabling it to spread along the MIEC wall with zero contact angle. MIEC materials include lithiated anode materials, unordered solid solutions with certain lithium atom mutual solubility, or metals that do not mix with lithium metal body phases but contain lithium diffusion phase boundary channels. ELI materials act as "inert adhesives" positioned at the interface between MIEC and SSE, maintaining contact between the SSE and MIEC. Without ELI, lithium metal deposition will commence from the root of MIEC, potentially leading to mechanical separation between the root of MIECs and SSEs.

In this study, an all-solid-state full cell was evaluated in terms of its performance with the MIEC tubules containing a minimal quantity of pre-deposited Li[77]. At 0.1 C [Figure 15B], this cell exhibited superior performance, exhibiting a lower overpotential (0.25 *vs.* 0.45 V), much higher discharge capacity (164 *vs.*

123 $mA{\cdot}h{\cdot}g^{-1}$), and significantly higher CE (99.83% *vs.* 82.22%). Furthermore, this full cell endured almost no deterioration throughout more than 50 cycles (in conformity with Figure 15C), and the specific gravimetric capacity of the Li/MIEC composite anode reached an exceptionally high value of approximately 900 $mA{\cdot}h{\cdot}g^{-1}$. Thus, these results validate the practical use of the MIEC architecture for applications in all-solid-state metal battery systems, which evolved from mechanistic notions to quantitative theory and ultimately to effective design application.

Despite the significant improvements achieved in enhancing stability and safety of lithium metal anodes by employing 3D nanostructures, the electrochemical Li deposition remains the primary source of Li in these anodes. Li-free substrates provoke Li depletion issues when combined with intercalation cathode materials, such as $LiCoO_2$ and $LiFePO_4$. Moreover, 3D substrates without preloaded Li cannot couple with high-capacity S and O_2 cathodes. To address these concerns, recent studies propose that utilizing preloaded lithium metal anodes created through a thermal infusion of Li into 3D nanostructured host materials[79], exhibiting greater attraction and efficacy for use in batteries, particularly those featuring non-lithiated cathode materials (S and O_2).

The utilization of a lithiophilic Si coating on a porous scaffold permits uniform coating of molten lithium metal on the surface of the matrix or encapsulation inside the 3D structure [Figure 16A and B], resulting in a considerable specific capacity of up to 2,300 $mAh{\cdot}g^{-1}$ as a stable lithium metal anode. Due to its reduced effective current density and ability to effectively accommodate Li volume variation, this groundbreaking electrode exhibits stable cycling performance over 80 cycles with lower overpotential (< 90 mV) at 3 $mA{\cdot}cm^{-2}$, which stands in stark contrast to bare Li foil[79].

A well-designed channel can guide Li-ion flux to move vertically along the electrode instead of parallelly, preventing uncontrolled Li deposition since the flux in each channel is mutually isolated[80]. An anode was proposed by Zhang *et al.* by adopting carbide wood (C-wood) as the substrate with preloaded lithium metal[81]. Low-pitched wood with channel structures ranging from 15 to 100 μm was employed, and its unique channel structure was well preserved after carbonization. The wetting between carbon and lithium metals is crucial for preparing lithium/carbon composite materials. To achieve this, Zhang *et al.* utilized a low-cost and simple method to cover a thin layer of ZnO on the channel walls of C-wood[81]. ZnO particles were formed and uniformly dispersed inside the channels. As expected, molten Li quickly rushed into the ZnO-coated channels, forming a brilliant lithium/C-wood composite material. This quick process was mainly due to the excellent reaction between lithium metal and ZnO and capillary forces generated by the hydrophilic surface. SEM was performed to investigate the morphological changes of the ZnO-coated-C-wood composite material. Figure 16C presents its typical channel structure, with channel sizes ranging from 5 to 60 μm and a groove wall thickness of ~1 μm. Such a formation resulted in a porous conductive framework capable of accommodating lithium metal (with a porosity rate of 73%) and maintaining optimal stability even after 230 cycles. This channel construction scheme holds immense potential in regulating lithium stripping/plating behavior.

Apart from conductive substrates, Liu *et al.* discovered that porous PI films, an electrically insulating material, can also accommodate molten Li injection[82]. This injected lithium metal serves as a conductive medium for electron transfer, and the exposed insulating surface following lithium peeling effectively prevents further Li deposition and dendrite formation. Experimental outcomes indicate that preloaded lithium in PI electrodes still exhibits a flat voltage profile, even at a high current density of 5 $mA{\cdot}cm^{-2}$ after 100 cycles[82].

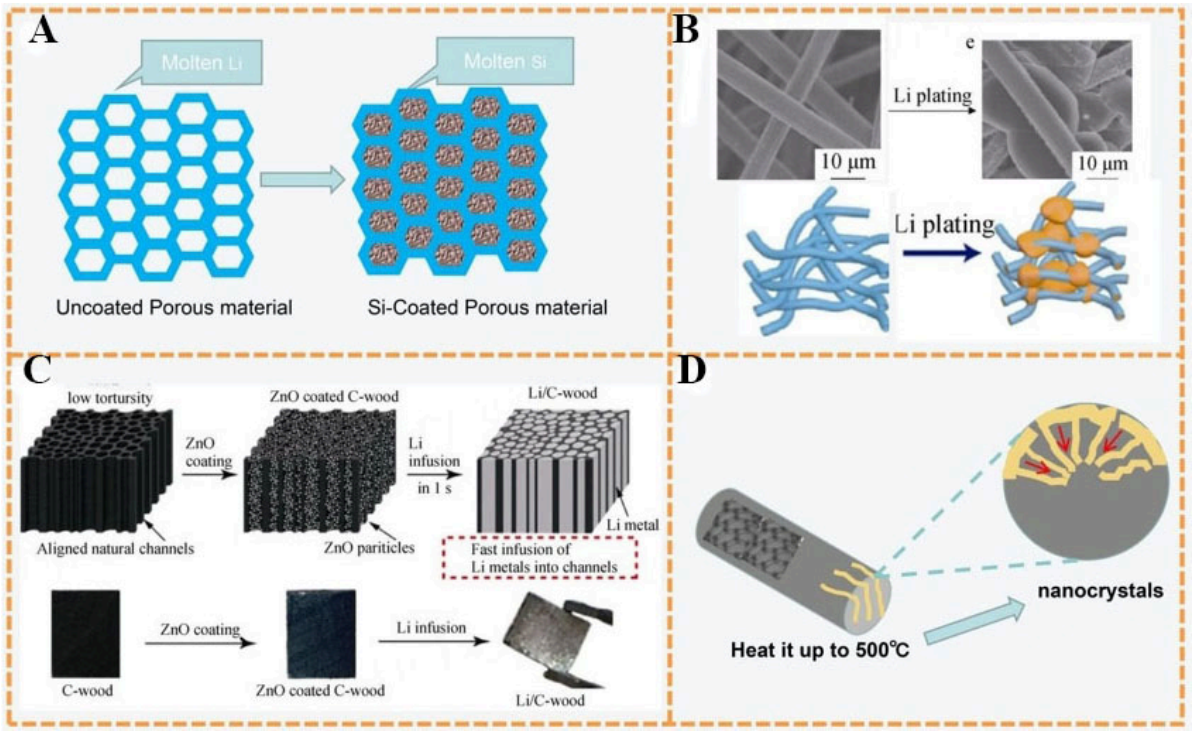

Figure 16. Design of 3D host structure with preloaded Li. Schematics and digital images of (A) Li infusion into the 3D porous host; (B) SEM image of Li infused in carbon nanofibers[79], Copyright 2017, Elsevier; (C) fabrication process from C-Wood (left) to ZnO-coated C-Wood (middle), and finally to Li/C-wood composite (right)[81]. Copyright 2017, National Academy of Science; (D) schematic illustration of the infusion process for impregnating the nanocrevasses of the carbon scaffold with Li. SEM: scanning electron microscopy.

The large specific surface area, mechanical strength, and lightweightness of carbon fibers render them exceptionally appealing for energy storage applications. Regretfully, their poor affinity for lithium metal poses a serious impediment to their viability as Li hosts. Consequently, initiatives have been instituted to enhance the surface features of carbon fibers. Go *et al.* uncovered that carbon fibers heated to 500 °C exhibited a wealth of nanocrystals, which furnished substantial capillary force to expedite the injection of molten Li into the carbon scaffold [Figure 16D], thus accelerating the construction of the 3D skeleton anodes[83].

A superb 3D composite anode

Recently, Lin *et al.* engineered an ultra-thin (≈50 μm) superb composite lithium anode through a spark reaction between Li and a layered reduced graphene oxide (rGO) film [Figure 17A][84]. Figure 17C compares the voltage distribution of a symmetric Li-rGO electrode cell and a bare Li foil cell after more than 100 cycles at 1 mA·cm^{-2}. Li-rGO exhibits a stable voltage curve with less hysteresis, whereas the Li foil experiences increasingly greater lag in the course of cycling. Further tests were conducted on the first, tenth, fiftieth, and hundredth cycles of the layered Li-rGO cell [Figure 17B]. Compared with the bare lithium electrode, there was no obvious increase in the flat voltage platform during charging and discharging states for layered Li-rGO.

The highly reduced polarization and stable cycling can be further supported by the electrochemical impedance spectroscopy (EIS) conducted on symmetric cells before cycling and after ten cycles [Figure 17E]. On the corresponding Nyquist plots, the semicircle at the high-frequency range is a good indicator of the interfacial resistance at SEI and the charge transfer resistance at the Li surface. Before

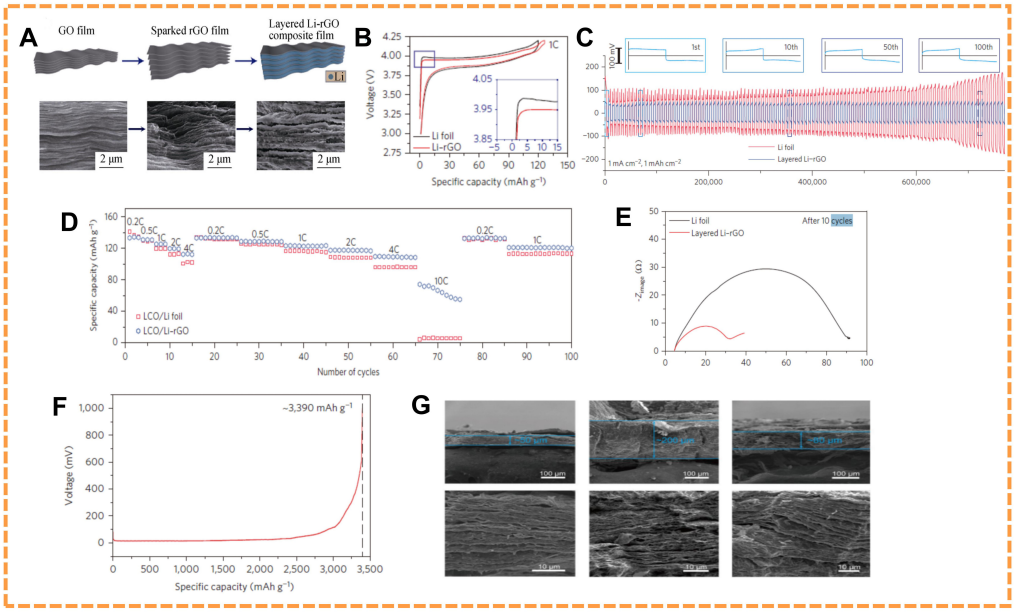

Figure 17. (A) rGO (left), sparked rGO (middle), and Li-rGO composite (right); (B) Voltage profile comparison of the LCO/Li-rGO cells and the LCO/Li foil cells at rates of 1 C; (C) Galvanostatic cycling of a symmetric Li-rGO electrode (blue) and bare Li foil (red); (D) Rate capability of the LCO/Li-rGO and LCO/Li foil cells (E) Nyquist plots of the symmetric cells after ten galvanostatic cycles; (F) Full Li stripping curve of the Li-rGO electrode; (G) Layered Li-rGO electrodes with different thicknesses[84]. Copyright 2016 Macmillan Publishers Limited.

cycling, the Li foil exhibited a high interfacial impedance (650 Ω), which decreased to 85 Ω. In contrast, the interfacial resistance of layered Li-rGO continuously dropped from 30 Ω before cycling to 25 Ω after ten cycles. This phenomenon suggests that layered Li-rGO can achieve better electrode stability and more favorable lithium stripping/plating kinetics. Notably, layered Li-rGO not only exhibits excellent electrochemical performance but also retains most of its capacity. An extractable capacity of 3390 mAh g^{-1} can be obtained when charged to 1 V [Figure 17F], which is very close to the theoretical capacity of pure lithium. The high specific capacity can be attributed to the lightweight and porocity of the rGO framework induced by the reduction, where the mass of the framework only accounts for 7 wt% of the entire electrode. SEM images of the Li-rGO electrodes with thicknesses of 50, 80, and 200 μm are shown in Figure 17G. The magnified SEM images indicate a consistent layered structure with similar spacing, despite the electrode thickness.

The present study reports the performance of the superb layered Li-rGO anodes in combination with lithium cobalt oxide (LCO) and lithium titanium oxide (LTO). Notably, the utilization of the Li-rGO anode design led to significantly improved rate capability and lower hysteresis compared to conventional Li foil cells. A higher LCO capacity was retained when utilizing Li-rGO anodes, particularly at high rates (110 mAh·g^{-1} at 4 C and 70 mAh·g^{-1} at 10 C, Figure 17D). In comparison, Li foil cells only offered a capacity of 95 mAh·g^{-1} and 5 mAh·g^{-1} at 4 C and 10 C, respectively. Interestingly, Li foil cells displayed consistently higher overpotential during the initial stage of charging, resulting in a 'bump' shape [Figure 17B], and this effect becomes more pronounced at increased rates. Notably, this is consistent with the behavior observed in symmetric Li foil cycling experiments. Collectively, these results demonstrate the improved power and stability inherent in utilizing layered Li-rGO designs[84]. The layering mechanism is not only found in electrode design but is also very common in battery separator modification.

SEPARATOR OPTIMIZATION

In response to the demand for improved safety performance in metal lithium batteries, many researchers have endeavored to optimize separator performance through modification. Traditional polypropylene (PP) separators, under high-temperature conditions, are prone to thermal shrinkage and pore formation, resulting in short circuits. Conversely, modified separators typically demonstrate enhanced thermal stability and are better equipped to withstand heat contraction at high temperatures. Modified separators not only require inhibition of ion migration between positive and negative electrode materials but also necessitate excellent wetting properties, low electrical resistance, and high flux. Porous structures and surface-active dyes are commonly employed in the modification of separator materials to improve pore sizes and wetting properties. The mechanical strength of separators is significantly relevant in safety issues, such as battery puncture, necessitating the consideration of mechanical performance in separator modification. Recent years have witnessed a plethora of studies focused on the optimization of lithium battery separators, which constitute the subject matter of the following section in this review.

Inorganic material/polymer hybrid-coated separators

Hybrid coatings composed of inorganic material and polymers are highly sought after for their unique advantages that arise from the combination of properties intrinsic to each component. It is widely anticipated that hybrid coatings will provide enhanced mechanical stability at high temperatures and improved electrolyte affinity in separators. One promising approach to accomplish this goal involves the coating of ordered poly(methyl methacrylate) (PMMA) and SiO_2 nanoparticles onto both sides of a PE separator[85]. The improved mechanical stability is attributed to the reinforcing effects of SiO_2, while the augmented wettability arises from the higher affinity of PMMA toward the electrolyte compared with the pure PE separator. As a result, the SiO_2@PMMA-coated PE separator exhibits superior rate capability and safety performance relative to its uncoated counterpart.

A ZrO_2/poly (acrylic acid) (PAA) coating was constructed on a plasma-activated PE separator with a layer-by-layer approach[86]. The PE substrate was carbodiimide-crosslinked with the ZrO_2/PAA coating. The thickness of the coating can be easily adjusted by altering the number of cycles within the layer-by-layer process. This composite separator integrates the advantages of functional polymers and inorganic nanoparticles and exhibits superior electrochemical and safety performance.

A thin poly(3,4-ethylenedioxythiophene)-co-poly(ethylene glycol) (PEDOT-PEG)/AlF_3 hybrid coating was applied onto a PE separator[87]. The ionic conductivity of the PEDOT-PEG phase in the coating provides practical benefits for the electrochemical performance of the separator. Incorporation of AlF_3 into the coating can aid in enhancing the thermal stability of the separator and stabilizing the electrolyte. Through a synergistic effect arising from the combination of these two components, the coated PE separator showed reduced thermal shrinkage and improved discharge capacity and cycling performance. To further optimize the separator performance, a SiO_2/PVDF hybrid nanofiber coating was applied to a PP non-woven separator[88]. Electrospinning a mixture containing PI and the corresponding filler followed by imidization was employed to develop SiO_2/PI and Al_2O_3/PI separators[89]. The composite separators exhibited superior thermal stability and mechanical strength.

Separators based on other polymers

PVDF can adsorb a substantial amount of electrolyte, which significantly contributes to battery performance[90]. The hydrophilic polymer HFP can be copolymerized with PVDF, further amplifying its affinity to electrolytes[91]. However, PVDF separators exhibit intrinsic weaknesses in tensile strength and thermal stability. To address these drawbacks, poly(m-phenylene isophthalamide) (PMIA), possessing both

remarkable mechanical properties and thermal stability, was implemented to create a tri-layer PVDF/PMIA/PVDF separator[92]. The battery using the PVDF/PMIA/PVDF separator showcased better discharge capacity and cycling stability compared with the cell utilizing the Celgard 2320 separator.

Polyvinyl alcohol (PVA), an immensely hydrophilic polymer, demonstrates strong adsorption characteristics towards electrolytes. A microporous PVA separator was meticulously produced by leveraging non-solvent-induced phase separation[93]. The PVA separator exhibits improved thermal stability relative to the PP separator. These features highlight the immense potential of the PVA separator in high-performance lithium batteries.

The performance of the separators with regard to the electrolyte was studied by examining their uptake and retention behaviors. The data presented in Figure 18C compare the electrolyte uptakes of the two separators. It was observed that the PVA separator displayed an electrolyte uptake of 170% after 15 min-almost double that of the PP separator (90%). Upon further inspection, both separators reached an equilibrium state after 2 h. At this time, the PVA separator demonstrated an electrolyte uptake of ~230%, outperforming its counterpart by a substantial 125%.

The current investigation provides a comprehensive analysis of the cycling performance of cells utilizing PVA and PP separators. Both cells demonstrated highly favorable cycling performances, with CEs remaining close to 100% after many cycles. Additionally, the PVA cell exhibited a higher discharge capacity than its PP counterpart. Furthermore, the capacity retention ratio of the PVA cell was determined to be ~97%, significantly greater than the PP cell (94%) after 50 cycles [Figure 18D]. To further characterize the stability of the PVA separator, SEM was conducted on the microstructure of the separator after cycling testing [Figure 18A and B]. Notably, minimal changes in separator morphology were observed before and after testing, which indicates the remarkable stability inherent to the use of the PVA separator design.

Figure 18E illustrates the evaluation of the wettability of the PP separator and the PVA separator via the liquid electrolyte contact angle. Results show the electrolyte droplets easily spread over a wide area of the PVA separator, demonstrating its quick wetness with the electrolyte. The PVA separator exhibits a contact angle of only 8.5°. Conversely, the PP separator is less wetted, with only an electrolyte droplet observed on its surface and exhibiting a contact angle of 42.4°. This significant discrepancy in electrolyte wettability verifies that the PVA porous separator is more electrolyte-philic than the PP separator, promoting the transport of Li^+.

Thermal shrinkage is another significant consideration for battery safety. The images of the PVA separator and the PP separator before and after exposure to 160 °C for 1 h are highly different. After thermal treatment, the PVA separator demonstrated superior thermal stability, showing virtually no dimensional change, while the PP separator underwent substantial thermal shrinkage of ~85%.

In summary, addressing the imperative necessity of improving safety performance in metal lithium batteries, separator modification has emerged as one salient research area gaining broad attention across the industry. Multiple strategies for separator modification will undoubtedly contribute to further enhancing safety and stability in metal lithium batteries.

CONCLUSIONS & PROSPECTS

Scientists have been engaged in a challenging pursuit for decades to resolve the issues associated with lithium anodes. With the increasing demand for high-energy-density energy storage devices, new

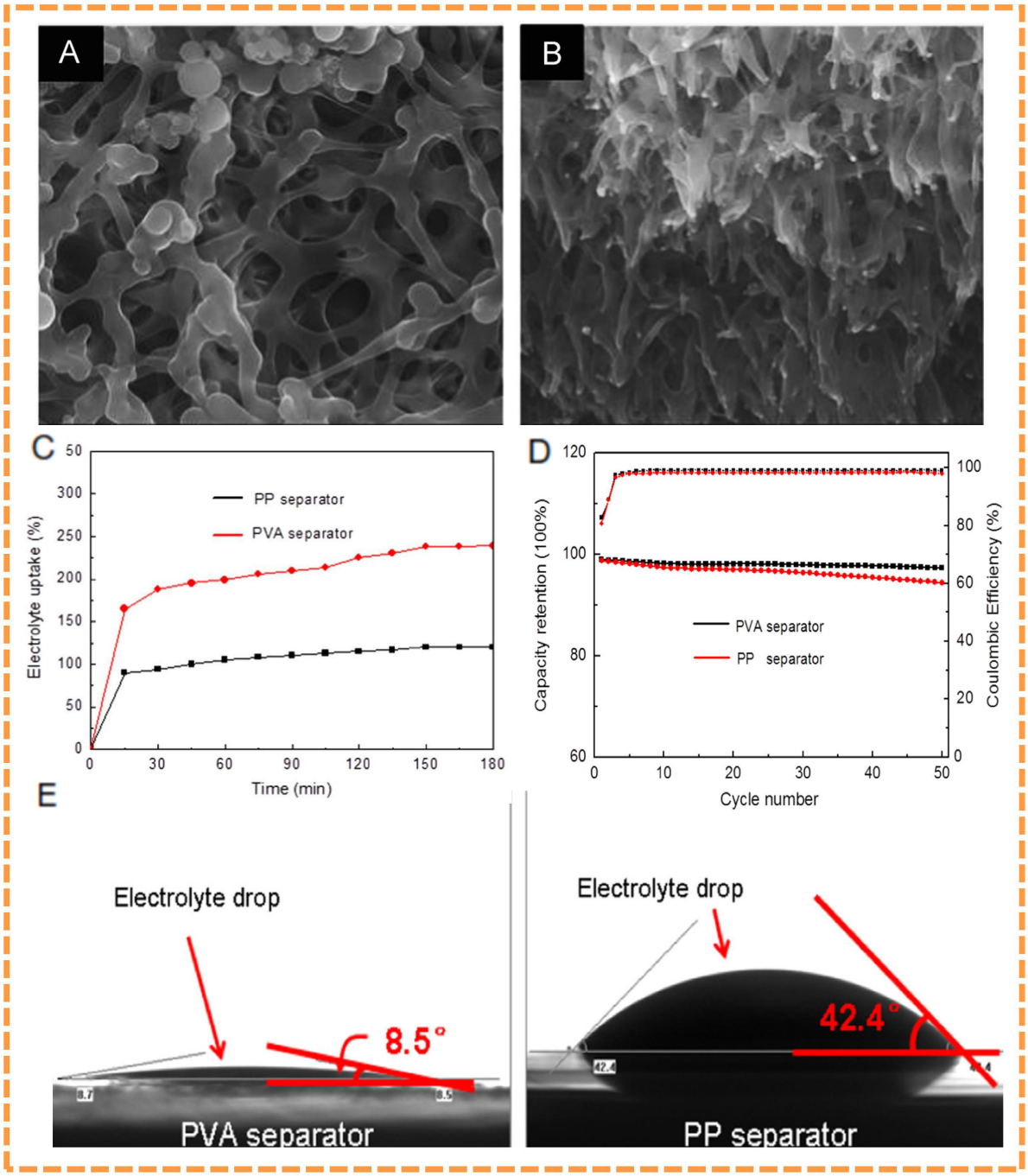

Figure 18. Surface (A) and cross-section (B) SEM images of the PVA separator after the cycling test. Electrolyte uptake (C) and retention (D) of PP separator and PVA separator. (E) Photograph showing liquid electrolyte wettability of different separators and the corresponding contact angle test results[93]. Copyright 2015, Elsevier. SEM: Scanning electron microscopy; PVA: polyvinyl alcohol.

opportunities and challenges are presented in the realm of lithium metal batteries. The present discourse endeavors to deliberate on the latest research developments of lithium anodes and puts forth various models to facilitate the comprehension of the fundamental mechanism of anode issues. A gamut of enhancement strategies is proffered for both the lithium metal anode and the electrolyte by prioritizing electrolyte optimization, electrolyte-electrode interface engineering, and electrode frame design.

An optimized electrolyte composition is a promising strategy for promoting high CEs and safety in lithium metal batteries by facilitating the formation of a high-performance SEI. The position and type of substitution groups in organic electrolyte components impact SEI composition. Immersion or *in situ* growth methods for the *in situ* SEI can help improve contact between the SEI and lithium metal anode. A promising alternative method for stabilizing the lithium anode is through inorganic/polymer hybrid solid electrolytes, which combine the advantages of both inorganic and polymer materials to achieve high Li^+ conductivity with moderate rigidity. Despite significant progress in enhancing the conductivity of SSEs, there remains a considerable gap between the ionic conductivities of solid- and liquid-state electrolytes. Research into conduction pathways of Li^+ in SSEs is therefore needed to establish the optimal pathway for Li^+ conduction. Furthermore, the development of thin-film SSEs may offer another solution to further improve ion conductivity. However, the film thickness may weaken the dendrite-inhibiting effect of the SSE, thereby compromising battery safety performance. Therefore, finding a balance between high ion conductivity and safety is crucial in commercializing lithium metal batteries successfully.

The optimization of current collectors is an essential aspect in developing advanced lithium-ion batteries. 3D frameworks can simultaneously reduce local current density and restrict volume changes in the anodes while satisfying requirements for large-scale industrial production, such as winding and solution casting processes. Notably, the design of porous structures of current collectors is one of the key factors that affect battery rate performance and capacity. However, the low CE caused by significant corrosion resulting from a large specific area of the current collector has impeded the development of this strategy. Therefore, a combination of multiple approaches is necessary to tackle the multifaceted challenges of lithium metal anodes. Incorporating additives with 3D current collector frameworks to reduce corrosion, dendrites, and volume expansion represents a promising strategy for enhancing CE and ensuring battery safety. Considerable efforts are necessary to explore and optimize these multi-strategy systems to make 3D current collectors a practical approach for next-generation lithium metal batteries.

There is a significant need for the wide adoption of experimental conditions that closely resemble practical applications and for narrowing the gap between research and practical applications. Conventional experimental conditions often deviate greatly from actual usage, as lithium metal batteries are typically tested at relatively low current densities ($\leq$ 1 mA cm^{-2}), thick lithium metal anodes (100-400 μm), and excessive electrolyte volumes (50 μL or more) under mild experimental conditions to avoid issues such as corrosion of metal lithium. This often leads to an overestimation of CE and safety performance that diverges significantly from actual application requirements. In practical scenarios, high current densities are employed, leading to substantially reduced lifetimes of only a few tens of cycles, which render these lithium metal batteries unsafe and unsuitable for industrial production applications due to the risks of short circuits and overheating. Therefore, laboratory research shall be coupled with realistic application testing to maximize the genuine meaning and applicability of laboratory work.

In conclusion, although there has been significant progress in developing modified anodes for lithium metal batteries, various strategies face formidable challenges in comprehensively enhancing both the electrochemical and safety performances. There is an urgent need for some integrated and comprehensive strategies to optimize electrochemical and safety performance of batteries. Research breakthroughs are crucial in helping reinvigorate the use of lithium metal anodes.

DECLARATIONS

Authors' contributions

Wrote the original manuscript: Cheng J, Gao W

Reviewing & editing: Kang S
Conception & supervision: Cui L

Availability of data and materials
Not applicable.

Financial support and sponsorship
This work was supported by the National Natural Science Foundation of China (51671136) and the Natural Science Foundation of Shanghai (23ZR1444100).

Conflicts of interest
All authors declared that there are no conflicts of interest.

Ethical approval and consent to participate
Not applicable.

Consent for publication
Not applicable.

REFERENCES
1. Shen X, Zhang R, Shi P, Chen X, Zhang Q. How does external pressure shape Li dendrites in Li metal batteries? *Adv Energy Mater* 2021;11:2003416. DOI
2. Lin D, Liu Y, Chen W, et al. Conformal lithium fluoride protection layer on three-dimensional lithium by nonhazardous gaseous reagent freon. *Nano Lett* 2017;17:3731-7. DOI
3. Kim US, Shin CB, Kim C. Effect of electrode configuration on the thermal behavior of a lithium-polymer battery. *J Power Sources* 2008;180:909-16. DOI
4. Xu G, Li J, Wang C, et al. The formation/decomposition equilibrium of Lih and its contribution on anode failure in practical lithium metal batteries. *Angew Chem Int Ed* 2021;60:7770-6. DOI PubMed
5. Kazyak E, Wang MJ, Lee K, et al. Understanding the electro-chemo-mechanics of Li plating in anode-free solid-state batteries with operando 3D microscopy. *Matter* 2022;5:3912-34. DOI
6. Dollé M, Sannier L, Beaudoin B, Trentin M, Tarascon J. Live scanning electron microscope observations of dendritic growth in lithium/polymer cells. *Electrochem Solid-State Lett* 2002;5:A286. DOI
7. Xu X, Liu Y, Kapitanova OO, Song Z, Sun J, Xiong S. Electro-chemo-mechanical failure of solid electrolytes induced by growth of internal lithium filaments. *Adv Mater* 2022;34:e2207232. DOI PubMed
8. Gao X, Zhou Y, Han D, et al. Thermodynamic understanding of Li-dendrite formation. *Joule* 2020;4:1864-79. DOI
9. Hong S, Kim J, Lim S, Yoon WY. Surface characterization of emulsified lithium powder electrode. *Electrochim Acta* 2004;50:535-9. DOI
10. Xiao Y, Xu R, Xu L, Ding J, Huang J. Recent advances in anion-derived SEIs for fast-charging and stable lithium batteries. *Energy Mater* 2022;1:100013. DOI
11. Chazalviel J. Electrochemical aspects of the generation of ramified metallic electrodeposits. *Phys Rev A* 1990;42:7355. DOI PubMed
12. Khurana R, Schaefer JL, Archer LA, Coates GW. Suppression of lithium dendrite growth using cross-linked polyethylene/poly(ethylene oxide) electrolytes: a new approach for practical lithium-metal polymer batteries. *J Am Chem Soc* 2014;136:7395-402. DOI PubMed
13. Zhang C, Liu S, Ma Z, Ranjith P. Combined micro-proppant and supercritical carbon dioxide (SC-CO_2) fracturing in shale gas reservoirs: a review. *Fuel* 2021;305:121431. DOI
14. Bai P, Li J, Brushett FR, Bazant MZ. Transition of lithium growth mechanisms in liquid electrolytes. *Energy Environ Sci* 2016;9:3221-9. DOI
15. Arakawa M, Tobishima S, Nemoto Y, Ichimura M, Yamaki J. Lithium electrode cycleability and morphology dependence on current density. *J Power Sources* 1993;43:27-35. DOI
16. Chen L, Fan X, Ji X, Chen J, Hou S, Wang C. High-energy Li metal battery with lithiated host. *Joule* 2019;3:732-44. DOI

17. Aryanfar A, Brooks DJ, Colussi AJ, Hoffmann MR. Quantifying the dependence of dead lithium losses on the cycling period in lithium metal batteries. *Phys Chem Chem Phys* 2014;16:24965-70. DOI PubMed
18. Qin K, Holguin K, Mohammadiroudbari M, et al. Strategies in structure and electrolyte design for high-performance lithium metal batteries. *Adv Funct Mater* 2021;31:2009694. DOI
19. Wood KN, Noked M, Dasgupta NP. Lithium metal anodes: toward an improved understanding of coupled morphological, electrochemical, and mechanical behavior. *ACS Energy Lett* 2017;2:664-72. DOI
20. Wang Q, Liu B, Shen Y, et al. Confronting the challenges in lithium anodes for lithium metal batteries. *Adv Sci* 2021;8:e2101111. DOI PubMed PMC
21. Lu D, Shao Y, Lozano T, et al. Failure mechanism for fast-charged lithium metal batteries with liquid electrolytes. *Adv Energy Mater* 2015;5:1400993. DOI
22. Cao W, Lu J, Zhou K, et al. Organic-inorganic composite SEI for a stable Li metal anode by *in-situ* polymerization. *Nano Energy* 2022;95:106983. DOI
23. Ye H, Zheng Z, Yao H, et al. Guiding uniform Li plating/stripping through lithium-aluminum alloying medium for long-life Li metal batteries. *Angew Chem Int Ed* 2019;131:1106-11. DOI
24. Li X, Zheng J, Ren X, et al. Dendrite-free and performance-enhanced lithium metal batteries through optimizing solvent compositions and adding combinational additives. *Adv Energy Mater* 2018;8:1703022. DOI
25. Ko J, Yoon YS. Recent progress in LiF materials for safe lithium metal anode of rechargeable batteries: is LiF the key to commercializing Li metal batteries? *Ceram Int* 2019;45:30-49. DOI
26. Monroe C, Newman J. The impact of elastic deformation on deposition kinetics at lithium/polymer interfaces. *J Electrochem Soc* 2005;152:A396. DOI
27. Zhang X, Xiang Q, Tang S, Wang A, Liu X, Luo J. Long cycling life solid-state Li metal batteries with stress self-adapted Li/garnet interface. *Nano Lett* 2020;20:2871-8. DOI
28. Bi Z, Guo X. Solidification for solid-state lithium batteries with high energy density and long cycle life. *Energy Mater* 2022;2:200011. DOI
29. Zheng ZJ, Ye H, Guo ZP. Recent progress in designing stable composite lithium anodes with improved wettability. *Adv Sci* 2020;7:2002212. DOI PubMed PMC
30. Huo H, Liang J, Zhao N, et al. Dynamics of the garnet/Li interface for dendrite-free solid-state batteries. *ACS Energy Lett* 2020;5:2156-64. DOI
31. Zhu P, Yan C, Dirican M, et al. $Li_{0.33}La_{0.557}TiO_3$ ceramic nanofiber-enhanced polyethylene oxide-based composite polymer electrolytes for all-solid-state lithium batteries. *J Mater Chem A* 2018;6:4279-85. DOI
32. Tu Z, Kambe Y, Lu Y, Archer LA. Nanoporous polymer-ceramic composite electrolytes for lithium metal batteries. *Adv Energy Mater* 2014;4:1300654. DOI
33. Zhou D, Liu R, He Y, et al. SiO_2 hollow nanosphere-based composite solid electrolyte for lithium metal batteries to suppress lithium dendrite growth and enhance cycle life. *Adv Energy Mater* 2016;6:1502214. DOI
34. Tikekar MD, Choudhury S, Tu Z, Archer LA. Design principles for electrolytes and interfaces for stable lithium-metal batteries. *Nat Energy* 2016:1:16114. DOI
35. Pan Q, Smith DM, Qi H, Wang S, Li CY. Hybrid electrolytes with controlled network structures for lithium metal batteries. *Adv Mater* 2015;27:5995-6001. DOI
36. Zhao Y, Wu C, Peng G, et al. A new solid polymer electrolyte incorporating $Li_{10}GeP_2S_{12}$ into a polyethylene oxide matrix for all-solid-state lithium batteries. *J Power Sources* 2016;301:47-53. DOI
37. Chen B, Huang Z, Chen X, et al. A new composite solid electrolyte PEO/$Li_{10}GeP_2S_{12}$/SN for all-solid-state lithium battery. *Electrochim Acta* 2016;210:905-14. DOI
38. Zhao Y, Huang Z, Chen S, et al. A promising PEO/LAGP hybrid electrolyte prepared by a simple method for all-solid-state lithium batteries. *Solid State Ion* 2016;295:65-71. DOI
39. Zhou W, Wang S, Li Y, Xin S, Manthiram A, Goodenough JB. Plating a dendrite-free lithium anode with a polymer/ceramic/polymer sandwich electrolyte. *J Am Chem Soc* 2016;138:9385-8. DOI
40. Lin D, Liu W, Liu Y, et al. High ionic conductivity of composite solid polymer electrolyte via *in situ* synthesis of monodispersed SiO_2 nanospheres in poly(ethylene oxide). *Nano Lett* 2016;16:459-65. DOI
41. Wang W, Yi E, Fici AJ, Laine RM, Kieffer J. Lithium ion conducting poly(ethylene oxide)-based solid electrolytes containing active or passive ceramic nanoparticles. *J Phys Chem C* 2017;121:2563-73. DOI
42. Liu W, Liu N, Sun J, et al. Ionic conductivity enhancement of polymer electrolytes with ceramic nanowire fillers. *Nano Lett* 2015;15:2740-5. DOI
43. Liu W, Lin D, Sun J, Zhou G, Cui Y. Improved lithium ionic conductivity in composite polymer electrolytes with oxide-ion conducting nanowires. *ACS Nano* 2016;10:11407-13. DOI PubMed
44. Fu KK, Gong Y, Dai J, et al. Flexible, solid-state, ion-conducting membrane with 3D garnet nanofiber networks for lithium batteries. *Proc Natl Acad Sci USA* 2016;113:7094-9. DOI PubMed PMC
45. Hagen M, Dörfler S, Althues H, et al. Lithium-sulphur batteries-binder free carbon nanotubes electrode examined with various electrolytes. *J Power Sources* 2012;213:239-48. DOI
46. Wang Q, Jin J, Wu X, Ma G, Yang J, Wen Z. A shuttle effect free lithium sulfur battery based on a hybrid electrolyte. *Phys Chem*

Chem Phys 2014;16:21225-9. DOI
47. Wang L, Wang Y, Xia Y. A high performance lithium-ion sulfur battery based on a Li_2S cathode using a dual-phase electrolyte. *Energy Environ Sci* 2015;8:1551-8. DOI
48. Yu X, Bi Z, Zhao F, Manthiram A. Hybrid lithium-sulfur batteries with a solid electrolyte membrane and lithium polysulfide catholyte. *ACS Appl Mater Interfaces* 2015;7:16625-31. DOI PubMed
49. Busche MR, Drossel T, Leichtweiss T, et al. Dynamic formation of a solid-liquid electrolyte interphase and its consequences for hybrid-battery concepts. *Nat Chem* 2016;8:426-34. DOI
50. Tsai CL, Roddatis V, Chandran CV, et al. $Li_7La_3Zr_2O_{12}$ interface modification for Li dendrite prevention. *ACS Appl Mater Interfaces* 2016;8:10617-26. DOI
51. Cai M, Lu Y, Su J, et al. In situ lithiophilic layer from H^+/Li^+ exchange on garnet surface for the stable lithium-solid electrolyte interface. *ACS Appl Mater Interfaces* 2019;11:35030-8. DOI PubMed
52. Shen K, Wang Z, Bi X, et al. Magnetic field-suppressed lithium dendrite growth for stable lithium-metal batteries. *Adv Energy Mater* 2019;9:1900260. DOI
53. Sheng O, Zheng J, Ju Z, et al. In situ construction of a LiF-enriched interface for stable all-solid-state batteries and its origin revealed by Cryo-TEM. *Adv Mater* 2020;32:e2000223. DOI PubMed
54. Aurbach D, Gofer Y, Ben-zion M, Aped P. The behaviour of lithium electrodes in propylene and ethylene carbonate: Te major factors that influence Li cycling efficiency. *J Electroanal Chem* 1992;339:451-71. DOI
55. Shiraishi S, Kanamura K, Takehara Z. Surface condition changes in lithium metal deposited in nonaqueous electrolyte containing HF by dissolution-deposition cycles. *J Electrochem Soc* 1999;146:1633. DOI
56. Zhang SS. Role of $LiNO_3$ in rechargeable lithium/sulfur battery. *Electrochim Acta* 2012;70:344-8. DOI
57. Vega JA, Zhou J, Kohl PA. Electrochemical comparison and deposition of lithium and potassium from phosphonium- and ammonium-TFSI ionic liquids. *J Electrochem Soc* 2009;156:A253. DOI
58. Morita M, Aoki S, Matsuda Y. Ac imepedance behaviour of lithium electrode in organic electrolyte solutions containing additives. *Electrochim Acta* 1992;37:119-23. DOI
59. Zhang X, Cheng X, Chen X, Yan C, Zhang Q. Fluoroethylene carbonate additives to render uniform Li deposits in lithium metal batteries. *Adv Funct Mater* 2017;27:1605989. DOI
60. Stark JK, Ding Y, Kohl PA. Dendrite-free electrodeposition and reoxidation of lithium-sodium alloy for metal-anode battery. *J Electrochem Soc* 2011;158:A1100. DOI
61. Han X, Gong Y, Fu KK, et al. Negating interfacial impedance in garnet-based solid-state Li metal batteries. *Nat Mater* 2017;16:572-9. DOI
62. van den Broek J, Afyon S, Rupp JLM. Interface-engineered all-solid-state Li-ion batteries based on garnet-type fast Li^+ conductors. *Adv Energy Mater* 2016;6:1600736. DOI
63. Luo W, Gong Y, Zhu Y, et al. Transition from superlithiophobicity to superlithiophilicity of garnet solid-state electrolyte. *J Am Chem Soc* 2016;138:12258-62. DOI
64. Wang C, Gong Y, Liu B, et al. Conformal, nanoscale ZnO surface modification of garnet-based solid-state electrolyte for lithium metal anodes. *Nano Lett* 2017;17:565-71. DOI
65. Xiao Z, Zhou NY, Wang X. et al. Dual-layered 3D composite skeleton enables spatially ordered lithium plating/stripping for lithium metal batteries with ultra-low N/P ratios. *ACS Appl Energy Mater* 2022;5:14071-80. DOI
66. Sun B, Fang M, Huang Z, Wu H. Robust current collector promoting the li metal anode cycling with appropriate interspaces. *J Electrochem Soc* 2018;165:A2026. DOI
67. Li C, Zhang X, Zhu Y, et al. Modulating the lithiophilicity at electrode/electrolyte interface for high-energy Li-metal batteries. *Energy Mater* 2022;1:100017. DOI
68. Xiong X, Qiao Q, Zhou Q, et al. Constructing a lithiophilic polyaniline coating via *in situ* polymerization for dendrite-free lithium metal anode. *Nano Res* 2023;16:8448-56. DOI
69. Wang T, Liu X, Wang Y, Fan L. High areal capacity dendrite-free Li anode enabled by metal-organic framework-derived nanorod array modified carbon cloth for solid state Li metal batteries. *Adv Funct Mater* 2021;31:2001973. DOI
70. Ji X, Liu D, Prendiville DG, Zhang Y, Liu X, Stucky GD. Spatially heterogeneous carbon-fiber papers as surface dendrite-free current collectors for lithium deposition. *Nano Today* 2012;7:10-20. DOI
71. Jin C, Sheng O, Luo J, et al. 3D lithium metal embedded within lithiophilic porous matrix for stable lithium metal batteries. *Nano Energy* 2017;37:177-86. DOI
72. Zhang R, Cheng XB, Zhao CZ, et al. Conductive nanostructured scaffolds render low local current density to inhibit lithium dendrite growth. *Adv Mater* 2016;28:2155-62. DOI
73. Lu LL, Ge J, Yang JN, et al. Free-standing copper nanowire network current collector for improving lithium anode performance. *Nano Lett* 2016;16:4431-7. DOI
74. Yang CP, Yin YX, Zhang SF, Li NW, Guo YG. Accommodating lithium into 3D current collectors with a submicron skeleton towards long-life lithium metal anodes. *Nat Commun* 2015;6:8058. DOI PubMed PMC
75. Yan K, Lu Z, Lee H, et al. Selective deposition and stable encapsulation of lithium through heterogeneous seeded growth. *Nat Energy* 2016;1:16010. DOI
76. Zhang Y, Liu B, Hitz E, et al. A carbon-based 3D current collector with surface protection for Li metal anode. *Nano Res*

2017;10:1356-65. DOI
77. Chen Y, Wang Z, Li X, et al. Li metal deposition and stripping in a solid-state battery via Coble creep. *Nature* 2020;578:251-5. DOI
78. Herring C. Diffusional viscosity of a polycrystalline solid. *J Appl Phys* 1950;21:437-45. DOI
79. Liu L, Yin Y, Li J, et al. Free-Standing hollow carbon fibers as high-capacity containers for stable lithium metal anodes. *Joule* 2017;1:563-75. DOI
80. Liu W, Lin D, Pei A, Cui Y. Stabilizing lithium metal anodes by uniform Li-ion flux distribution in nanochannel confinement. *J Am Chem Soc* 2016;138:15443-50. DOI PubMed
81. Zhang Y, Luo W, Wang C, et al. High-capacity, low-tortuosity, and channel-guided lithium metal anode. *Proc Natl Acad Sci USA* 2017;114:3584-9. DOI
82. Liu Y, Lin D, Liang Z, Zhao J, Yan K, Cui Y. Lithium-coated polymeric matrix as a minimum volume-change and dendrite-free lithium metal anode. *Nat Commun* 2016;7:10992. DOI PubMed PMC
83. Go W, Kim MH, Park J, et al. Nanocrevasse-rich carbon fibers for stable lithium and sodium metal anodes. *Nano Lett* 2019;19:1504-11. DOI
84. Lin D, Liu Y, Liang Z, et al. Layered reduced graphene oxide with nanoscale interlayer gaps as a stable host for lithium metal anodes. *Nat Nanotechnol* 2016;11:626-32. DOI
85. Liao C, Wang W, Han L, et al. A flame retardant sandwiched separator coated with ammonium polyphosphate wrapped by SiO_2 on commercial polyolefin for high performance safety lithium metal batteries. *Appl Mater Today* 2020;21:100793. DOI
86. Xu L, Daphne Ma XY, Wang W, Liu J, Wang Z, Lu X. Polymeric one-side conductive janus separator with preferably oriented pores for enhancing lithium metal battery safety. *J Mater Chem A* 2021;9:3409-17. DOI
87. Liao C, Wang W, Wang J, et al. Magnetron sputtering deposition of silicon nitride on polyimide separator for high-temperature lithium-ion batteries. *J Energy Chem* 2021;56:1-10. DOI
88. Kim S, Kang HS, Sohn E, Chang B, Park IJ, Lee SG. High discharge energy density and efficiency in newly designed PVDF@SiO_2-PVDF composites for energy capacitors. *ACS Appl Energy Mater* 2020;3:8937-45. DOI
89. Shayapat J, Chung OH, Park JS. Electrospun polyimide-composite separator for lithium-ion batteries. *Electrochim Acta* 2015;170:110-21. DOI
90. Kang G, Cao Y. Application and modification of poly(vinylidene fluoride) (PVDF) membranes - a review. *J Membr Sci* 2014;463:145-65. DOI
91. Wang W, Yuen ACY, Yuan Y, et al. Nano architectured halloysite nanotubes enable advanced composite separator for safe lithium metal batteries. *Chem Eng J* 2023;451:138496. DOI
92. Wang W, Yuan Y, Wang J, et al. Enhanced electrochemical and safety performance of lithium metal batteries enabled by the atom layer deposition on PVDF-HFP separator. *ACS Appl Energy Mater* 2019;2:4167-74. DOI
93. Xiao W, Zhao L, Gong Y, Liu J, Yan C. Preparation and performance of poly(vinyl alcohol) porous separator for lithium-ion batteries. *J Membr Sci* 2015;487:221-8. DOI